Mathematical and computational modeling for the generation and propagation of waves in marine and coastal environments

Maria Kazolea

School of Environmental Engineering Technical University of Crete

September 27, 2013

European Union
European Social Fund

OPERATIONAL PROGRAMME
EDUCATION AND LIFELONG LEARNING
investing in knowledge society
MINISTRY OF EDUCATION & RELIGIOUS AFFAIRS, CULTURE & SPORTS
MANAGING AUTHORITY

NSRF 2007-2013
programme for development
EUROPEAN SOCIAL FUND

Co-financed by Greece and the European Union

Motivation

Discretize **depth-integrated** equations that model free surface flows, using mass and momentum conservation, by (unstructured) FV schemes.

- Most popular (applied): Nonlinear Shallow Water Equations (SWE)

Motivation

Discretize **depth-integrated** equations that model free surface flows, using mass and momentum conservation, by (unstructured) FV schemes.

- Most popular (applied): Nonlinear Shallow Water Equations (SWE)
  - Limitation: Not applicable for wave propagation in intermediate / deeper waters (dispersion has an effect on free surface flow)
- Popular Boussinesq-type (BT) models for **intermediate water** depths:
  - Peregrine's standard equations (1967) but for $\frac{h}{L} \approx \frac{1}{5}$

Motivation

Discretize **depth-integrated** equations that model free surface flows, using mass and momentum conservation, by (unstructured) FV schemes.

- Most popular (applied): Nonlinear Shallow Water Equations (SWE)
  - Limitation: Not applicable for wave propagation in intermediate / deeper waters (dispersion has an effect on free surface flow)
- Popular Boussinesq-type (BT) models for **intermediate water** depths:
  - Peregrine's standard equations (1967) but for $\frac{h}{L} \approx \frac{1}{5}$
  - Madsen and Sörensen's (MS) equations (1992)
  - Nowgu's equations (1993) for $\frac{h}{L} \approx \frac{1}{2}$
  - Beji and Nadaoka (BN) equations (1996)

Motivation

Discretize **depth-integrated** equations that model free surface flows, using mass and momentum conservation, by (unstructured) FV schemes.

- Most popular (applied): Nonlinear Shallow Water Equations (SWE)
  - Limitation: Not applicable for wave propagation in intermediate / deeper waters (dispersion has an effect on free surface flow)
- Popular Boussinesq-type (BT) models for **intermediate water** depths:
  - Peregrine's standard equations (1967) but for $\frac{h}{L} \approx \frac{1}{5}$
  - Madsen and Sörensen's (MS) equations (1992)
  - Nowgu's equations (1993) for $\frac{h}{L} \approx \frac{1}{2}$
  - Beji and Nadaoka (BN) equations (1996)
  - Gobbi, Kirby and Wei BT model (2000)
  - Variety of BT models that include higher-order nonlinear and dispersive terms: P.A. Madsen et al. (2002-2009), Lynett et al. (2004-2010).

(Some) Numerical Works

- Until recently, **Finite-Differences** (FD) was the predominant method based on the work of Wei & Kirby (1995), for 1D & 2D computations

(Some) Numerical Works

- Until recently, **Finite-Differences** (FD) was the predominant method based on the work of Wei & Kirby (1995), for 1D & 2D computations
- More recently **hybrid FV/FD** schemes in 1D & 2D:
  - Nwogu's, MS, BN, Serre Green-Green Naghdi S-GN equations using: Riemann solvers (Roe's and HLL-type), MUSCL-type reconstructions. Erduran et al. (2005 & 2007), Cienfuegos et al (2006 & 2007), Tonelli & Petti (2009), Shiach & Mingham (2009), Roeber et al. (2010), Bonneton et al. (2010), Kazolea & Delis (2011), Dutykh et al. (2011).

(Some) Numerical Works

- Until recently, **Finite-Differences** (FD) was the predominant method based on the work of Wei & Kirby (1995), for 1D & 2D computations
- More recently **hybrid FV/FD** schemes in 1D & 2D:
  - Nwogu's, MS, BN, Serre Green-Green Naghdi S-GN equations using: Riemann solvers (Roe's and HLL-type), MUSCL-type reconstructions. Erduran et al. (2005 & 2007), Cienfuegos et al (2006 & 2007), Tonelli & Petti (2009), Shiach & Mingham (2009), Roeber et al. (2010), Bonneton et al. (2010), Kazolea & Delis (2011), Dutykh et al. (2011).
  - MS equations in 2D Tonelli & Petti (2009 & 2010), two-layer BT equations Lynnet et al., (2006-2010), TVD Boussinesq solver Shi, Kirby et. al. (2012).

(Some) Numerical Works

- Until recently, **Finite-Differences** (FD) was the predominant method based on the work of Wei & Kirby (1995), for 1D & 2D computations
- More recently **hybrid FV/FD** schemes in 1D & 2D:
  - Nwogu's, MS, BN, Serre Green-Green Naghdi S-GN equations using: Riemann solvers (Roe's and HLL-type), MUSCL-type reconstructions. Erduran et al. (2005 & 2007), Cienfuegos et al (2006 & 2007), Tonelli & Petti (2009), Shiach & Mingham (2009), Roeber et al. (2010), Bonneton et al. (2010), Kazolea & Delis (2011), Dutykh et al. (2011).
  - MS equations in 2D Tonelli & Petti (2009 & 2010), two-layer BT equations Lynnet et al., (2006-2010), TVD Boussinesq solver Shi, Kirby et. al. (2012).
- 2D **Finite Element** (FE) on unstructured meshes: Walkey & Berzins (2002), Sorensen et al. (2004), Escilsson & Sherwin (2006) and Engsig-Karup et al. (2008).

(Some) Numerical Works

- Until recently, **Finite-Differences** (FD) was the predominant method based on the work of Wei & Kirby (1995), for 1D & 2D computations
- More recently **hybrid FV/FD** schemes in 1D & 2D:
  - Nwogu's, MS, BN, Serre Green-Green Naghdi S-GN equations using: Riemann solvers (Roe's and HLL-type), MUSCL-type reconstructions. Erduran et al. (2005 & 2007), Cienfuegos et al (2006 & 2007), Tonelli & Petti (2009), Shiach & Mingham (2009), Roeber et al. (2010), Bonneton et al. (2010), Kazolea & Delis (2011), Dutykh et al. (2011).
  - MS equations in 2D Tonelli & Petti (2009 & 2010), two-layer BT equations Lynnet et al., (2006-2010), TVD Boussinesq solver Shi, Kirby et. al. (2012).
- 2D **Finite Element** (FE) on unstructured meshes: Walkey & Berzins (2002), Sorensen et al. (2004), Escilsson & Sherwin (2006) and Engsig-Karup et al. (2008).
- **FV for unstructured meshes**: Only one work by Asmar and Nwogu (2006) using a low-order staggered scheme

Outline

- Physical problem set up

Outline

- Physical problem set up
- Discretization of Nwogu's and Madsen and Sørensen's extened BT models in 1D
- Numerical results in 1D

Outline

- Physical problem set up
- Discretization of Nwogu's and Madsen and Sørensen's extened BT models in 1D
- Numerical results in 1D
- Comparison of two 2D FV schemes on triangles

Outline

- Physical problem set up
- Discretization of Nwogu's and Madsen and Sørensen's extened BT models in 1D
- Numerical results in 1D
- Comparison of two 2D FV schemes on triangles
- A new unstructured FV scheme for BT equations
- Numerical results in 2D

Outline

- Physical problem set up
- Discretization of Nwogu's and Madsen and Sørensen's extened BT models in 1D
- Numerical results in 1D
- Comparison of two 2D FV schemes on triangles
- A new unstructured FV scheme for BT equations
- Numerical results in 2D
- Conclusions

Physical problem setup

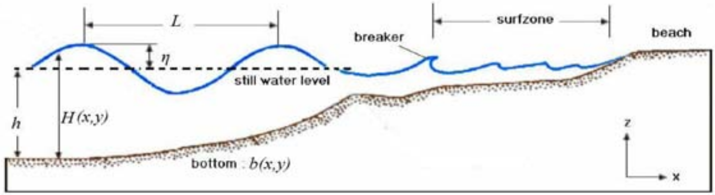

η: **free surface elevation**;
h: **steel water level**;
$H = \eta + h$: **total water depth**;
b: **bottom topography**;
L: **wave length**;
A: **wave amplitude**

Deep water: $\frac{h}{L} > \frac{1}{2}$

Intermediate water: $\frac{1}{20} < \frac{h}{L} \leq \frac{1}{2}$

Shallow water: $\frac{h}{L} \leq \frac{1}{20}$

Physical problem setup

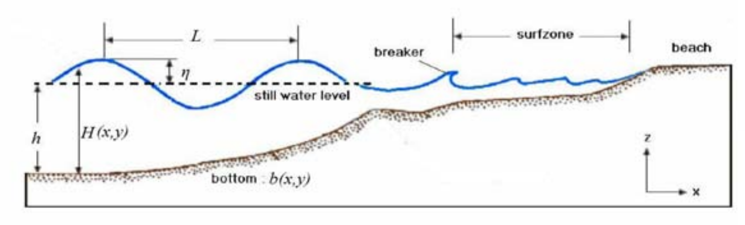

η: **free surface elevation**;

h: **steel water level**;

$H = \eta + h$: **total water depth**;

b: **bottom topography**;

L: **wave length**;

A: **wave amplitude**

Deep water: $\frac{h}{L} > \frac{1}{2}$

Intermediate water: $\frac{1}{20} < \frac{h}{L} \leq \frac{1}{2}$

Shallow water: $\frac{h}{L} \leq \frac{1}{20}$

Mathematical models: Nwogu's equations

Vector conservative form (for both models):

$$\mathbf{U}_t + \mathbf{F}(\mathbf{U}^\star)_x = \mathbf{S}(\mathbf{U}), \tag{1}$$

$$\mathbf{U} = \begin{bmatrix} H \\ P^* \end{bmatrix}, \ \mathbf{F}(\mathbf{U}) = \begin{bmatrix} Hu \\ Hu^2 + \frac{1}{2}gH^2 \end{bmatrix}, \ \mathbf{U}^\star = \begin{bmatrix} H \\ Hu \end{bmatrix}.$$

Using $z_a = 0.53753h$ as optimal reference depth (Roeber et al., 2010).

Mathematical models: Nwogu's equations

Vector conservative form (for both models):

$$\mathbf{U}_t + \mathbf{F}(\mathbf{U}^\star)_x = \mathbf{S}(\mathbf{U}), \tag{1}$$

$$\mathbf{U} = \begin{bmatrix} H \\ P^* \end{bmatrix}, \ \mathbf{F}(\mathbf{U}) = \begin{bmatrix} Hu \\ Hu^2 + \frac{1}{2}gH^2 \end{bmatrix}, \ \mathbf{U}^\star = \begin{bmatrix} H \\ Hu \end{bmatrix}.$$

Using $z_a = 0.53753h$ as optimal reference depth (Roeber et al., 2010).

- $P^* = Hu + Hz_a\left(\frac{z_a}{2}u_{xx} + (hu)_{xx}\right)$ [**"Velocity" function**]

Mathematical models: Nwogu's equations

Vector conservative form (for both models):

$$\mathbf{U}_t + \mathbf{F}(\mathbf{U}^\star)_x = \mathbf{S}(\mathbf{U}), \tag{1}$$

$$\mathbf{U} = \begin{bmatrix} H \\ P^* \end{bmatrix}, \ \mathbf{F}(\mathbf{U}) = \begin{bmatrix} Hu \\ Hu^2 + \frac{1}{2}gH^2 \end{bmatrix}, \ \mathbf{U}^\star = \begin{bmatrix} H \\ Hu \end{bmatrix}.$$

Using $z_a = 0.53753h$ as optimal reference depth (Roeber et al., 2010).

- $P^* = Hu + Hz_a\left(\frac{z_a}{2}u_{xx} + (hu)_{xx}\right)$ ["Velocity" function]
- $\mathbf{S}(\mathbf{U}) = \mathbf{S_b} + \mathbf{S_f} + \mathbf{S_d}$ [Source terms]

Mathematical models: Nwogu's equations

Vector conservative form (for both models):

$$\mathbf{U}_t + \mathbf{F}(\mathbf{U}^\star)_x = \mathbf{S}(\mathbf{U}), \tag{1}$$

$$\mathbf{U} = \begin{bmatrix} H \\ P^* \end{bmatrix}, \quad \mathbf{F}(\mathbf{U}) = \begin{bmatrix} Hu \\ Hu^2 + \frac{1}{2}gH^2 \end{bmatrix}, \quad \mathbf{U}^\star = \begin{bmatrix} H \\ Hu \end{bmatrix}.$$

Using $z_a = 0.53753h$ as optimal reference depth (Roeber et al., 2010).

- $P^* = Hu + Hz_a\left(\frac{z_a}{2}u_{xx} + (hu)_{xx}\right)$ [**"Velocity" function**]
- $\mathbf{S}(\mathbf{U}) = \mathbf{S_b} + \mathbf{S_f} + \mathbf{S_d}$ [**Source terms**]

$\mathbf{S_b} = [0 \quad -gHb_x]^T$, $\mathbf{S_f} = [0 \quad -gHS_f]$, $\mathbf{S_d} = [-\psi_C \quad -u\psi_C + \psi_M - R_b]$

$S_f = n_m^2 \frac{u|u|}{H^{-4/3}}$ Friction force, $n_m =$ Manning coeff.

Mathematical models: Nwogu's equations

Vector conservative form (for both models):

$$\mathbf{U}_t + \mathbf{F}(\mathbf{U}^\star)_x = \mathbf{S}(\mathbf{U}), \tag{1}$$

$$\mathbf{U} = \begin{bmatrix} H \\ P^* \end{bmatrix}, \; \mathbf{F}(\mathbf{U}) = \begin{bmatrix} Hu \\ Hu^2 + \frac{1}{2}gH^2 \end{bmatrix}, \; \mathbf{U}^\star = \begin{bmatrix} H \\ Hu \end{bmatrix}.$$

Using $z_a = 0.53753h$ as optimal reference depth (Roeber et al., 2010).

- $P^* = Hu + Hz_a\left(\frac{z_a}{2}u_{xx} + (hu)_{xx}\right)$ ["Velocity" function]
- $\mathbf{S}(\mathbf{U}) = \mathbf{S_b} + \mathbf{S_f} + \mathbf{S_d}$ [Source terms]

$\mathbf{S_b} = [0 \quad -gHb_x]^T$, $\mathbf{S_f} = [0 \quad -gHS_f]$, $\mathbf{S_d} = [-\psi_C \quad -u\psi_C + \psi_M - R_b]$

$S_f = n_m^2 \frac{u|u|}{H^{-4/3}}$ Friction force, $n_m =$ Manning coeff.

- $\psi_M = H_t z_a\left(\frac{z_a}{2}u_{xx} + (hu)_{xx}\right)$, $\psi_C = \left[\left(\frac{z_a^2}{2} - \frac{h^2}{6}\right)hu_{xx} + \left(z_a + \frac{h}{2}\right)h(hu)_{xx}\right]_x$
- R_b parametrization of wave breaking characteristics

Mathematical models: Madsen & Sørensen's equations

- $P^* = Hu - (B + \frac{1}{3})h^2(Hu)_{xx} - \frac{1}{3}h_x(Hu)_x$ ["Velocity" function]

Mathematical models: Madsen & Sørensen's equations

- $P^* = Hu - (B + \frac{1}{3})h^2(Hu)_{xx} - \frac{1}{3}h_x(Hu)_x$ ["Velocity" function]
- $\mathbf{S}(\mathbf{U}) = \mathbf{S_b} + \mathbf{S_f} + \mathbf{S_d}$ [Source term]

where now $\mathbf{S_d} = [0 \quad -\psi - R_b]$ and

Mathematical models: Madsen & Sørensen's equations

- $P^* = Hu - (B + \frac{1}{3})h^2(Hu)_{xx} - \frac{1}{3}h_x(Hu)_x$ ["Velocity" function]

- $\mathbf{S}(\mathbf{U}) = \mathbf{S_b} + \mathbf{S_f} + \mathbf{S_d}$ [Source term]

where now $\mathbf{S_d} = [0 \quad -\psi - R_b]$ and

- $\psi = -Bgh^3\eta_{xxx} - 2h^2 h_x Bg\eta_{xx}$

$B = \frac{1}{15}$ determines the dispersion properties of the system.

Numerical Model

- Advective part and topography source: Well-balanced FV formulation
  Dispersive terms: Finite differences.

Numerical Model

- Advective part and topography source: Well-balanced FV formulation
  Dispersive terms: Finite differences.

- Roe's Riemann solver is used (Roe, 1981).

Numerical Model

- Advective part and topography source: Well-balanced FV formulation
  Dispersive terms: Finite differences.

- Roe's Riemann solver is used (Roe, 1981).

- Upwinding of the topography source term (Bermudez et al., 1994, Delis et al., 2008).

Numerical Model

- Advective part and topography source: Well-balanced FV formulation
  Dispersive terms: Finite differences.

- Roe's Riemann solver is used (Roe, 1981).

- Upwinding of the topography source term (Bermudez et al., 1994, Delis et al., 2008).

- High-order spatial accuracy: fourth order **MUSCL**-type scheme (Yamamoto et al., 1998).

Numerical Model

- Advective part and topography source: Well-balanced FV formulation
  Dispersive terms: Finite differences.
- Roe's Riemann solver is used (Roe, 1981).
- Upwinding of the topography source term (Bermudez et al., 1994, Delis et al., 2008).
- High-order spatial accuracy: fourth order **MUSCL**-type scheme (Yamamoto et al., 1998).
- For dispersive terms: fourth order FD of first-order spatial derivatives, second and third-order FD for second and third-order derivatives.
- Satisfy the *C*-property (flow at rest) to higher spatial order: Addition of an extra term to bed upwinding (Hubbard and Garcia-Navarro, 2000 and Delis and Nikolos, 2009)

Numerical Model (cont.)

- Special treatment wet/dry fronts:
  - Identify dry cells: through a tolerance parameter
  - *Consistent depth reconstruction*: satisfy $\frac{\partial h}{\partial x} = -\frac{\partial b}{\partial x}$ to high-order on wet/dry fronts
  - *Satisfy an extended C-property*: Redefinition of the bed slope, numerical fluxes are computed assuming temporarily zero velocity at wet/dry faces (Brufau et al., 2004)
- **Time Integration** (should at least match the order of truncation errors from dispersion terms): Third order Adams-Basforth predictor and fourth-order Adams-Moulton corrector stage.

Numerical Model (cont.)

- Special treatment wet/dry fronts:
  - Identify dry cells: through a tolerance parameter
  - *Consistent depth reconstruction*: satisfy $\frac{\partial h}{\partial x} = -\frac{\partial b}{\partial x}$ to high-order on wet/dry fronts
  - *Satisfy an extended C-property*: Redefinition of the bed slope, numerical fluxes are computed assuming temporarily zero velocity at wet/dry faces (Brufau et al., 2004)
- **Time Integration** (should at least match the order of truncation errors from dispersion terms): Third order Adams-Basforth predictor and fourth-order Adams-Moulton corrector stage.
- Extract depth averaged velocities, u, from the ”velocities” functions P^* by solving a tridiagonal system,

Numerical Model (cont.)

- Special treatment wet/dry fronts:
  - Identify dry cells: through a tolerance parameter
  - *Consistent depth reconstruction*: satisfy $\frac{\partial h}{\partial x} = -\frac{\partial b}{\partial x}$ to high-order on wet/dry fronts
  - *Satisfy an extended C-property*: Redefinition of the bed slope, numerical fluxes are computed assuming temporarily zero velocity at wet/dry faces (Brufau et al., 2004)
- **Time Integration** (should at least match the order of truncation errors from dispersion terms): Third order Adams-Basforth predictor and fourth-order Adams-Moulton corrector stage.
- Extract depth averaged velocities, u, from the "velocities" functions P^* by solving a tridiagonal system, Thomas algorithm.

Numerical Test & Results in 1D: (Solitary wave propagation)

Two cases: $A/ = 0.1$ $Dx = 0.05$ $C_r = 0.4$ (MS left, Nwogu's right)

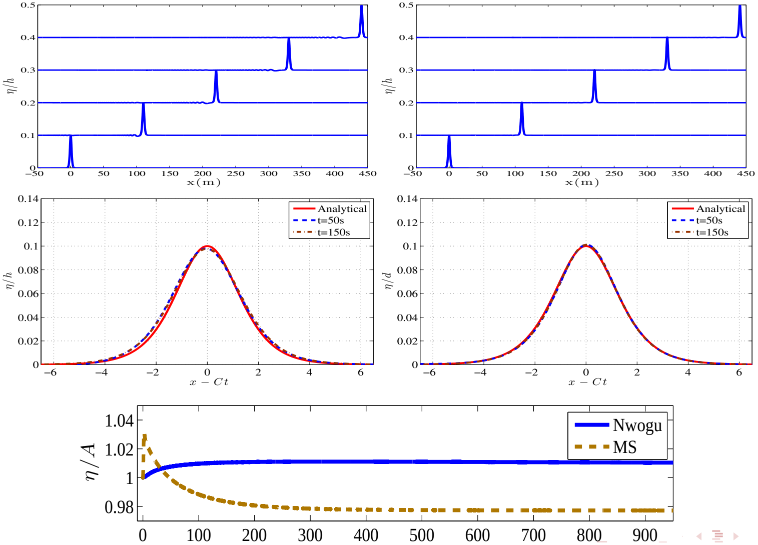

Solitary wave propagation

Two cases: $A/h = 0.2$ $Dx = 0.05$ $C_r = 0.4$ (MS left, Nwogu's right)

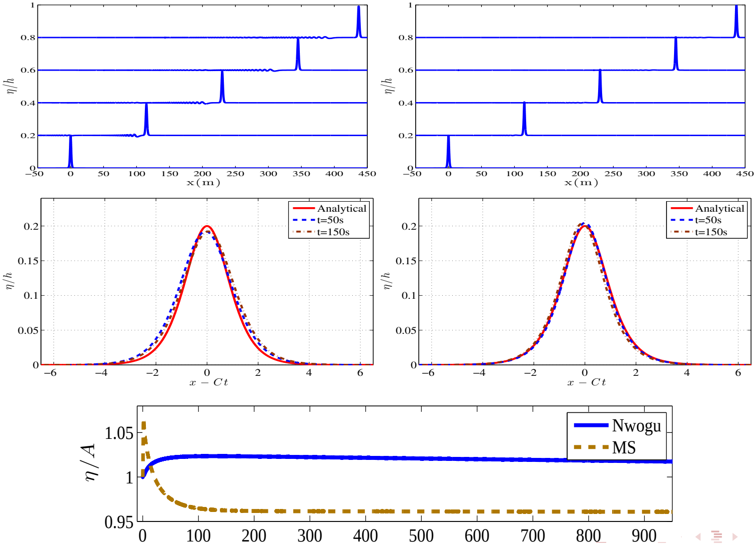

Head on collision of two solitary waves

$$A/h = 0.3 \; Dx = 0.1m \; C_r = 0.4, \;\; x \in [0, 300]$$

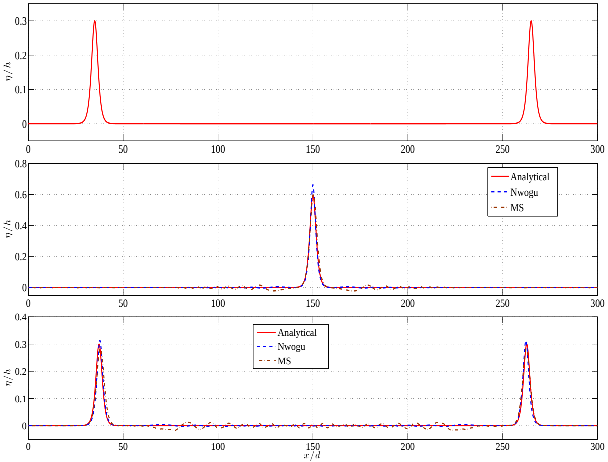

Regular wave propagation over a submerged bar

$$T = 2.02s, \; H = 0.02, h/L = 0.11, Dx = 0.04m$$

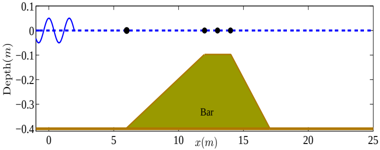

Regular wave propagation over a submerged bar

$$T = 2.02s,\ H = 0.02, h/L = 0.11, Dx = 0.04m$$

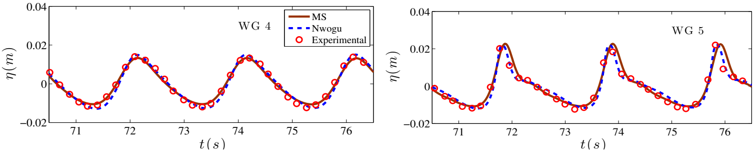

Regular wave propagation over a submerged bar

$T = 2.02s,\ H = 0.02, h/L = 0.11, Dx = 0.04m$

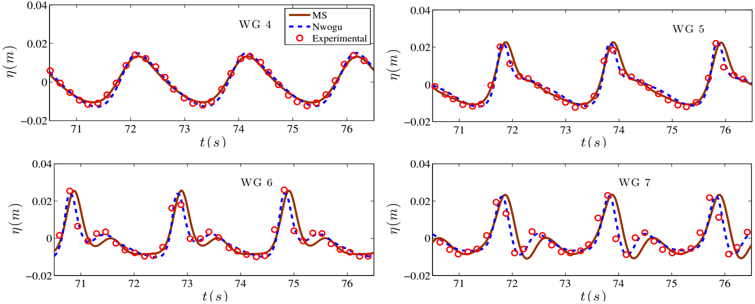

Regular wave propagation over a submerged bar

$T = 2.02s,\ H = 0.02, h/L = 0.11, Dx = 0.04m$

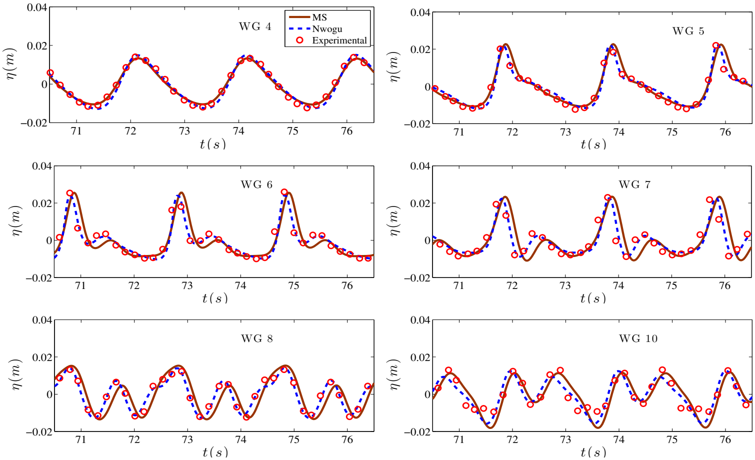

Mathematical Model: The NSWE

$$\frac{\partial \mathbf{U}}{\partial t} + \nabla \cdot \mathcal{H}(\mathbf{U}) = \mathcal{L}(\mathbf{U}) \text{ on } \Omega \times [0,t] \subset \mathbb{R}^2 \times \mathbb{R}^+,$$

$$\mathbf{U} = \begin{bmatrix} H \\ Hu \\ Hv \end{bmatrix}, \mathcal{H}(\mathbf{U}) = [\mathbf{F},\mathbf{G}] = \begin{bmatrix} Hu & Hv \\ Hu^2 + \frac{1}{2}gH^2 & Huv \\ Huv & Hv^2 + \frac{1}{2}gh^2 \end{bmatrix},$$

$$\mathcal{L}(\mathbf{U}) = [\mathbf{R}^1 + \mathbf{R}^2 + \mathbf{S_b}]$$

$$\mathbf{R}^1 = \begin{bmatrix} 0 & -gH\frac{\partial b(x,y)}{\partial x} & 0 \end{bmatrix}^{\mathrm{T}} \text{ and } \mathbf{R}^2 = \begin{bmatrix} 0 & 0 & -gH\frac{\partial b(x,y)}{\partial y} \end{bmatrix}^{\mathrm{T}}.$$

$$\mathbf{S} = \begin{bmatrix} 0 & -gHS_x^f & -gHS_y^f \end{bmatrix}^{\mathrm{T}} \quad \text{with}$$

$$S_x^f = \frac{n_m^2 u\|\mathbf{u}\|}{H^{\frac{4}{3}}} \quad \text{and} \quad S_y^f = \frac{n_m^2 v\|\mathbf{u}\|}{H^{\frac{4}{3}}},$$

NCFV approach

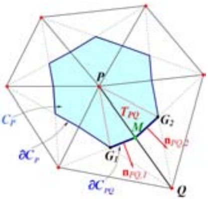

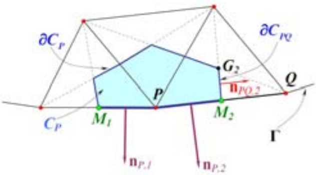

$$\iint_{C_P} \frac{\partial \mathbf{U}}{\partial t} d\Omega + \iint_{C_P} \nabla \cdot \mathcal{H} d\Omega = \iint_{C_P} \mathbf{S} d\Omega \;\Rightarrow\; \frac{\partial}{\partial t} \iint_{C_P} \mathbf{U} d\Omega + \oint_{\partial C_P} \mathcal{H} \cdot \tilde{\mathbf{n}} dl = \iint_{C_P} \mathbf{S} d\Omega$$

NCFV approach

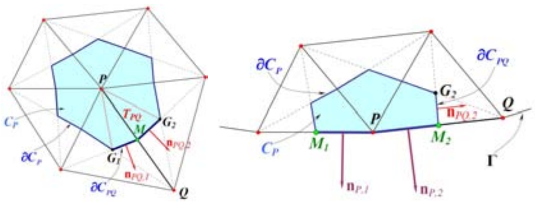

$$\iint_{C_P} \frac{\partial \mathbf{U}}{\partial t} d\Omega + \iint_{C_P} \nabla \cdot \mathcal{H} d\Omega = \iint_{C_P} \mathbf{S} d\Omega \Rightarrow \frac{\partial}{\partial t} \iint_{C_P} \mathbf{U} d\Omega + \oint_{\partial C_P} \mathcal{H} \cdot \tilde{\mathbf{n}} dl = \iint_{C_P} \mathbf{S} d\Omega$$

Introducing the flux vectors

$$\mathbf{\Phi}_{PQ} = \int_{\partial C_{PQ}} \left(\mathbf{F} \tilde{n}_x + \mathbf{G} \tilde{n}_y \right) dl \quad \text{and} \quad \mathbf{\Phi}_{P,\Gamma} = \int_{\partial C_P \cap \Gamma} \left(\mathbf{F} \tilde{n}_x + \mathbf{G} \tilde{n}_y \right) dl$$

Hence, FV scheme reads

$$\frac{\partial \mathbf{U}_P}{\partial t} = -\frac{1}{|C_P|} \sum_{Q \in K_P} \mathbf{\Phi}_{PQ} - \frac{1}{|C_P|} \mathbf{\Phi}_{P,\Gamma} + \frac{1}{|C_P|} \iint_{C_P.} (\mathbf{S}_b + \mathbf{S}_d + \mathbf{S}_f) d\Omega$$

NCFV approach

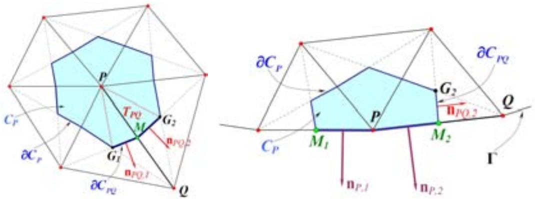

$$\iint_{C_P} \frac{\partial \mathbf{U}}{\partial t} d\Omega + \iint_{C_P} \nabla \cdot \mathcal{H} d\Omega = \iint_{C_P} \mathbf{S} d\Omega \Rightarrow \frac{\partial}{\partial t} \iint_{C_P} \mathbf{U} d\Omega + \oint_{\partial C_P} \mathcal{H} \cdot \widetilde{\mathbf{n}} dl = \iint_{C_P} \mathbf{S} d\Omega$$

Introducing the flux vectors

$$\mathbf{\Phi}_{PQ} = \int_{\partial C_{PQ}} \left(\mathbf{F} \tilde{n}_x + \mathbf{G} \tilde{n}_y \right) dl \quad \text{and} \quad \mathbf{\Phi}_{P,\Gamma} = \int_{\partial C_P \cap \Gamma} \left(\mathbf{F} \tilde{n}_x + \mathbf{G} \tilde{n}_y \right) dl$$

Hence, FV scheme reads

$$\frac{\partial \mathbf{U}_P}{\partial t} = -\frac{1}{|C_P|} \sum_{Q \in K_P} \mathbf{\Phi}_{PQ} - \frac{1}{|C_P|} \mathbf{\Phi}_{P,\Gamma} + \frac{1}{|C_P|} \iint_{C_P.} (\mathbf{S}_b + \mathbf{S}_d + \mathbf{S}_f) d\Omega$$

$\mathbf{\Phi}_{PQ}$ **Numerical flux**

NCFV approach: Gradient & divergence formulas

Green -Gauss linear reconstruction on Ω_P

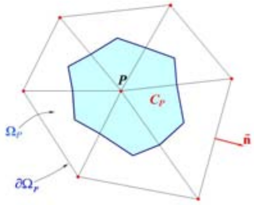

$$|C_P| = \frac{1}{3}|\Omega_P|$$

$$\iint_{\Omega_P} \nabla w dA = \oint_{\partial\Omega_P} w\tilde{\mathbf{n}} dl \Rightarrow$$

$$(\nabla w)_P = \frac{1}{|C_P|} \sum_{Q \in K_P} \frac{1}{2}\Big(w_P + w_Q\Big)\mathbf{n}_{PQ}$$

NCFV approach: Gradient & divergence formulas

Green -Gauss linear reconstruction on Ω_P

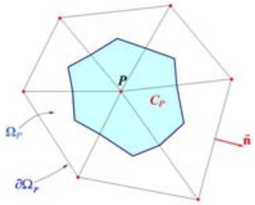

$$|C_P| = \frac{1}{3}|\Omega_P|$$

$$\iint_{\Omega_P} \nabla w dA = \oint_{\partial\Omega_P} w\tilde{\mathbf{n}} dl \Rightarrow$$

$$(\nabla w)_P = \frac{1}{|C_P|} \sum_{Q\in K_P} \frac{1}{2}\Big(w_P + w_Q\Big)\mathbf{n}_{PQ}$$

$$\iint_{\Omega_P} \nabla\cdot\mathbf{u} d\Omega = \oint_{\partial\Omega_P} \mathbf{u}\cdot\tilde{\mathbf{n}} dl = \sum_{Q\in K_P} \frac{3}{2}(\mathbf{u}_P + \mathbf{u}_Q)\cdot\mathbf{n}_{PQ} \Rightarrow$$

$$(\nabla\cdot\mathbf{u})_P = \frac{1}{2|C_P|} \sum_{Q\in K_P} (\mathbf{u}_P + \mathbf{u}_Q)\cdot\mathbf{n}_{PQ}$$

NCFV approach: Gradient & divergence formulas

Green -Gauss linear reconstruction on Ω_P

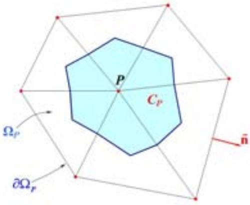

$$|C_P| = \frac{1}{3}|\Omega_P|$$

$$\iint_{\Omega_P} \nabla w dA = \oint_{\partial\Omega_P} w\tilde{\mathbf{n}} dl \Rightarrow$$

$$(\nabla w)_P = \frac{1}{|C_P|} \sum_{Q \in K_P} \frac{1}{2}\Big(w_P + w_Q\Big)\mathbf{n}_{PQ}$$

NCFV approach: Gradient & divergence formulas

Green -Gauss linear reconstruction on Ω_P

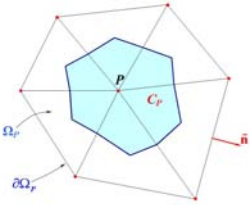

$$|C_P| = \frac{1}{3}|\Omega_P|$$

$$\iint_{\Omega_P} \nabla w dA = \oint_{\partial\Omega_P} w\tilde{\mathbf{n}} dl \Rightarrow$$

$$(\nabla w)_P = \frac{1}{|C_P|}\sum_{Q\in K_P}\frac{1}{2}\Big(w_P + w_Q\Big)\mathbf{n}_{PQ}$$

$$w^L_{i,PQ} = w_{i,P} + \frac{1}{2}\mathrm{LIM}\Big((\nabla w_i)^{upw}_P \cdot \mathbf{r}_{PQ}, (\nabla w_i)^{cent} \cdot \mathbf{r}_{PQ}\Big)$$

$$w^R_{i,PQ} = w_{i,Q} - \frac{1}{2}\mathrm{LIM}\Big((\nabla w_i)^{upw}_Q \cdot \mathbf{r}_{PQ}, (\nabla w_i)^{cent} \cdot \mathbf{r}_{PQ}\Big)$$

$$(\nabla w_i),^{cent} \cdot \mathbf{r}_{PQ} = w_{i,Q} - w_{i,P}, \ (\nabla w_i)_P,^{upw} \cdot \mathbf{r}_{PQ} = 2(\nabla w_i)_P - (\nabla w_i)^{cent}$$

CCFV approach

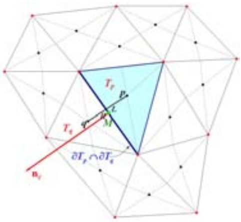

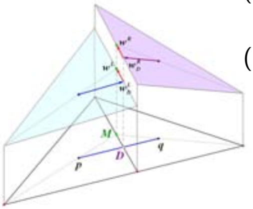

$$\frac{\partial \mathbf{U}_p}{\partial t}|T_p| = \sum_{q \in K(p)} \mathbf{\Phi}_q + \iint_{T_p} \mathbf{S} d\Omega.$$

$\mathbf{\Phi}_q$ **Numerical flux.**

Linear reconstruction

- Naive calculation (at point D)

$$(w_{i,p})_D^L = w_{i,p} + \frac{||\mathbf{r}_{pD}||}{||\mathbf{r}_{pq}||} \text{LIM}\left((\nabla w_i)_p^{\text{upw}} \cdot \mathbf{r}_{pq}, (\nabla w_i)^{\text{cent}} \cdot \mathbf{r}_{pq}\right);$$

$$(w_{i,q})_D^R = w_{i,q} - \frac{||\mathbf{r}_{Dq}||}{||\mathbf{r}_{pq}||} \text{LIM}\left((\nabla w_i)_q^{\text{upw}} \cdot \mathbf{r}_{pq}, (\nabla w_i)^{\text{cent}} \cdot \mathbf{r}_{pq}\right),$$

CCFV approach

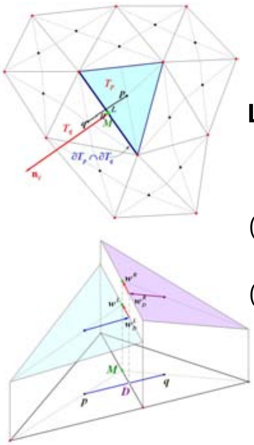

$$\frac{\partial \mathbf{U}_p}{\partial t}|T_p| = \sum_{q\in K(p)} \mathbf{\Phi}_q + \iint_{T_p} \mathbf{S}\, d\Omega.$$

$\mathbf{\Phi}_q$ **Numerical flux.**

Linear reconstruction

- Naive calculation (at point D)

$$\begin{aligned}(w_{i,p})_D^L &= w_{i,p} + \frac{\|\mathbf{r}_{pD}\|}{\|\mathbf{r}_{pq}\|}\mathrm{LIM}\left((\nabla w_i)_p^{\mathrm{upw}}\cdot \mathbf{r}_{pq}, (\nabla w_i)^{\mathrm{cent}}\cdot \mathbf{r}_{pq}\right);\\ (w_{i,q})_D^R &= w_{i,q} - \frac{\|\mathbf{r}_{Dq}\|}{\|\mathbf{r}_{pq}\|}\mathrm{LIM}\left((\nabla w_i)_q^{\mathrm{upw}}\cdot \mathbf{r}_{pq}, (\nabla w_i)^{\mathrm{cent}}\cdot \mathbf{r}_{pq}\right),\end{aligned}$$

- Corrected calculation (at point M) (Delis et al., 2011)

$$\begin{aligned}w_{i,p}^L &= (w_{i,p})_D^L + \mathbf{r}_{DM}\cdot(\nabla w_i)_p,\\ w_{i,q}^R &= (w_{i,q})_D^R + \mathbf{r}_{DM}\cdot(\nabla w_i)_q.\end{aligned}$$

CCFV approach: Gradient formulas

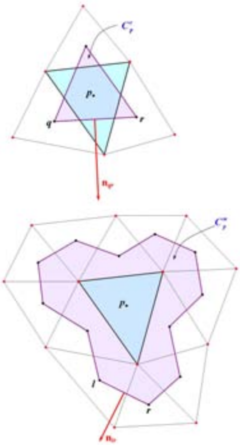

Three element (compact stencil) gradient

$$\nabla w_{i,p} = \frac{1}{|C_p^c|} \sum_{\substack{q,r \in K(p) \\ r \neq q}} \frac{1}{2}(w_{i,q} + w_{i,r})\mathbf{n}_{q,r}$$

Extended element (wide stencil) gradient

$$\nabla w_{i,p} = \frac{1}{|C_p^w|} \sum_{\substack{l,r \in K'(p) \\ r \neq l}} \frac{1}{2}\Big(w_{i,l} + w_{i,r}\Big)\mathbf{n}_{lr}$$

CCFV approach: Gradient formulas

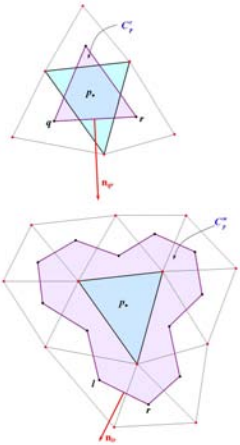

Three element (compact stencil) gradient

$$\nabla w_{i,p} = \frac{1}{|C_p^c|} \sum_{\substack{q,r \in K(p) \\ r \neq q}} \frac{1}{2}(w_{i,q} + w_{i,r})\mathbf{n}_{q,r}$$

Extended element (wide stencil) gradient

$$\nabla w_{i,p} = \frac{1}{|C_p^w|} \sum_{\substack{l,r \in K'(p) \\ r \neq l}} \frac{1}{2}\left(w_{i,l} + w_{i,r}\right)\mathbf{n}_{lr}$$

⋆ **Boundary conditions**: use the theory of characteristics for weak formulation for the NCFV and ghost cells for CCFV scheme

Topography source discretization

- Wel-ballanced schemes $\Rightarrow$ introduce topography source flux vectors $\mathbf{S}_{\mathbf{b}}^{-}$:

$$\iint_{T_p} \mathbf{S}_{\mathbf{b}}(\mathbf{U}^{\star})dxdy = \sum_{q\in K(p)} \mathbf{S}_{\mathbf{b}q}^{-} \quad \text{(CCFV)}$$

$$\iint_{C_P} \mathbf{S}_{\mathbf{b}}(\mathbf{U}^{\star})dxdy = \sum_{Q\in K_P} \mathbf{S}_{\mathbf{b}PQ}^{-} \quad \text{(NCFV)}$$

- $\mathbf{S}_{\mathbf{b}}{}^{-} = \frac{1}{2}\widetilde{\mathbf{P}}\left(\mathbf{I} - |\widetilde{\mathbf{\Lambda}}|\widetilde{\mathbf{\Lambda}}^{-1}\right)\widetilde{\mathbf{P}}^{-1}\widetilde{\mathbf{S}_{\mathbf{b}}}$ where (for 1st order scheme):

$$\widetilde{\mathbf{S}_{\mathbf{b}}}\,|_q = \begin{bmatrix} 0 \\ -g\dfrac{H^L+H^R}{2}\left(b^R-b^L\right)n_{qx} \\ -g\dfrac{H^L+H^R}{2}\left(b^R-b^L\right)n_{qy} \end{bmatrix}_q \quad \widetilde{\mathbf{S}_{\mathbf{b}}}\,|_{PQ} = \begin{bmatrix} 0 \\ -g\dfrac{H^L+H^R}{2}\left(b^R-b^L\right)n_{PQx} \\ -g\dfrac{H^L+H^R}{2}\left(b^R-b^L\right)n_{PQy} \end{bmatrix}_{PQ}$$

Topography source discretization

- Wel-ballanced schemes $\Rightarrow$ introduce topography source flux vectors $\mathbf{S}_\mathbf{b}^-$:

$$\iint_{T_p} \mathbf{S}_\mathbf{b}(\mathbf{U}^\star)dxdy = \sum_{q\in K(p)} \mathbf{S}_{\mathbf{b}q}^- \quad \text{(CCFV)}$$

$$\iint_{C_P} \mathbf{S}_\mathbf{b}(\mathbf{U}^\star)dxdy = \sum_{Q\in K_P} \mathbf{S}_{\mathbf{b}PQ}^- \quad \text{(NCFV)}$$

- $\mathbf{S_b}^- = \frac{1}{2}\widetilde{\mathbf{P}}\left(\mathbf{I} - |\widetilde{\mathbf{\Lambda}}|\widetilde{\mathbf{\Lambda}}^{-1}\right)\widetilde{\mathbf{P}}^{-1}\widetilde{\mathbf{S}_\mathbf{b}} + \mathbf{S}_\mathbf{b}^\star$ /2nd order scheme, **correction** term

$$\mathbf{S_b}^\star\,|_q = \begin{bmatrix} 0 \\ -g\dfrac{H^L + H_p}{2}\left(b^L - b_p\right)n_{qx} \\ -g\dfrac{H^L + H_p}{2}\left(b^L - b_p\right)n_{qy} \end{bmatrix} \quad \mathbf{S_b}^\star\,|_{PQ} = \begin{bmatrix} 0 \\ -g\dfrac{H^L + H_P}{2}\left(b^L - b_P\right)n_{PQx} \\ -g\dfrac{H^L + H_P}{2}\left(b^L - b_P\right)n_{PQy} \end{bmatrix}.$$

Topography source discretization (wet/dry)

- Extended C-property, (Castro et al, 2005)
- In the MUSCL scheme for hydrostatic conditions we must have, at i-cell

$$b^L - b_i = -(h^L - h_i) \quad \Rightarrow \quad (\nabla B)_i = -(\nabla h)_i$$

  - **If in the gradient calculation, of a wet cell, a dry node is involved we correct the h^L and/or h^R by imposing**

$$h^L = h_i - (b^L - b_i) \;\text{ and/or }\; h^R = h_j - (b^R - b_j)$$

- Redefine the bed value in the dry node for emerging bed situations in $\widetilde{\mathbf{S_b}}$ to maintain hydrostatic conditions, (Brufau et al, 2002).
- For water in motion over emerging slopes: If $h^L > \epsilon_{wd}$ and $h^R \leq \epsilon_{wd}$ and $h^L < (b^B - b^L)$, set temporarily for the wet i-cell $u^L = v^L = 0$

Numerical Results

Grids used:

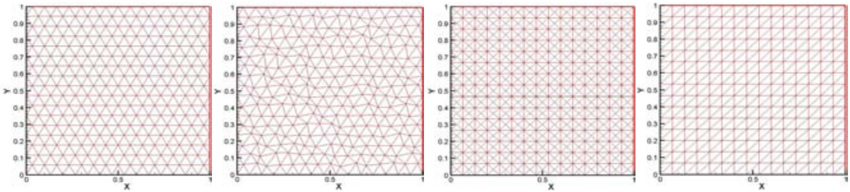

- **Consistently refined** grids, for N =degrees of freedom, characteristic length $h_N = \sqrt{L_x \times L_y / N}$
- Equivalent meshes

Scheme	Description
NCFV	Node-Centered FV Scheme
CCFVc1	Cell-Centered FV compact (naive) reconstruction stencil
CCFVc2	Cell-Centered FV compact reconstruction stencil (corrected)
CCFVw1	Cell-Centered FV wide (naive) reconstruction stencil
CCFVw2	Cell-Centered FV wide reconstruction stencil (corrected)

The traveling vortex solution

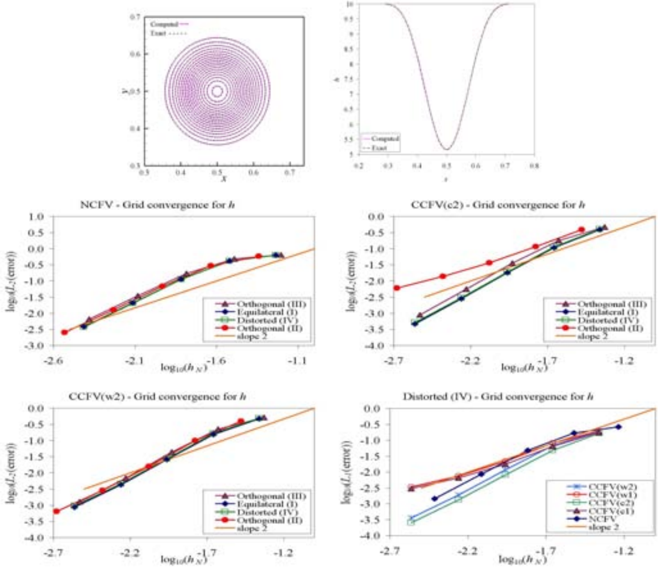

Traveling vortex: Convergence results

Comparison

1. **Convergence behavior** to second order: NCFV is not grid dependent/ CCFV depents on the grid used.

Comparison

1. **Convergence behavior** to second order: NCFV is not grid dependent/ CCFV depents on the grid used.
2. **Edge based limiting procedure** in the MUSCL reconstruction: inadequate for the CCFV schemes if the proposed correction not used.

Comparison

1. **Convergence behavior** to second order: NCFV is not grid dependent/ CCFV depents on the grid used.
2. **Edge based limiting procedure** in the MUSCL reconstruction: inadequate for the CCFV schemes if the proposed correction not used.
3. CCFVw2 has an almost identical behavior with the NCFV scheme is achieved, but with the extra **computational** cost introduced.

Comparison

1. **Convergence behavior** to second order: NCFV is not grid dependent/ CCFV depents on the grid used.
2. **Edge based limiting procedure** in the MUSCL reconstruction: inadequate for the CCFV schemes if the proposed correction not used.
3. CCFVw2 has an almost identical behavior with the NCFV scheme is achieved, but with the extra **computational** cost introduced.
4. Ghost cells for the boundary treatment in CCFV formulations can lead to an **order reduction**.

Comparison

1. **Convergence behavior** to second order: NCFV is not grid dependent/ CCFV depents on the grid used.
2. **Edge based limiting procedure** in the MUSCL reconstruction: inadequate for the CCFV schemes if the proposed correction not used.
3. CCFVw2 has an almost identical behavior with the NCFV scheme is achieved, but with the extra **computational** cost introduced.
4. Ghost cells for the boundary treatment in CCFV formulations can lead to an **order reduction**.
5. **Wet/dry treatment**: accurate for both FV approaches on all grid types.

Comparison

1. **Convergence behavior** to second order: NCFV is not grid dependent/ CCFV depents on the grid used.
2. **Edge based limiting procedure** in the MUSCL reconstruction: inadequate for the CCFV schemes if the proposed correction not used.
3. CCFVw2 has an almost identical behavior with the NCFV scheme is achieved, but with the extra **computational** cost introduced.
4. Ghost cells for the boundary treatment in CCFV formulations can lead to an **order reduction**.
5. **Wet/dry treatment**: accurate for both FV approaches on all grid types.

An unstructured FV scheme for BT Equations

Vector conservative form for Nwogu's equations:

$$\frac{\partial \mathbf{U}}{\partial t} + \nabla \cdot \mathcal{H}(\mathbf{U}^{\star}) = \mathcal{L}(\mathbf{U}^{\star}) \text{ on } \Omega \times [0,t] \subset \mathbb{R}^2 \times \mathbb{R}^+,$$

$\mathbf{U}$ vector of the **new variables**, $\mathbf{U}^{\star} = [H, Hu, Hv]^{\mathrm{T}}$ and $\mathcal{H} = [\mathbf{F}, \mathbf{G}]$

$$\mathbf{U} = \begin{bmatrix} H \\ P_1 \\ P_2 \end{bmatrix}, \mathcal{L}(\mathbf{U}) = [\mathbf{S_b} + \mathbf{S_d} + \mathbf{S_f}]$$

with $\mathbf{P} = \begin{bmatrix} P_1 \\ P_2 \end{bmatrix} = H\left[\frac{z_a^2}{2}\nabla(\nabla \cdot \mathbf{u}) + z_a \nabla(\nabla \cdot h\mathbf{u}) + \mathbf{u}\right]$ and

$$\mathbf{S_b} = \begin{bmatrix} 0 \\ -gHb_x \\ -gHb_y \end{bmatrix}, \quad \mathbf{S_d} = \begin{bmatrix} -\psi_c \\ -u\psi_c + \psi_{M_x} \\ -v\psi_c + \psi_{M_y} \end{bmatrix}, \quad \mathbf{S_f} = \begin{bmatrix} 0 \\ S_x^f + R_{b_x} \\ S_y^f + R_{b_y} \end{bmatrix}$$

Vector conservative form (cont.)

$$\psi_c = \nabla \cdot \left[\left(\frac{z_a^2}{2} - \frac{h^2}{6} \right) h \nabla (\nabla \cdot \mathbf{u}) + \left(z_a + \frac{h}{2} \right) h \nabla (\nabla \cdot h\mathbf{u}) \right]$$

$$\psi_{\mathbf{M}} = \begin{bmatrix} \psi_{M_x} \\ \psi_{M_y} \end{bmatrix} = H_t \frac{z_a^2}{2} \nabla (\nabla \cdot \mathbf{u}) + H_t z_a \nabla (\nabla \cdot h\mathbf{u})$$

Vector conservative form (cont.)

$$\psi_c = \nabla\cdot\left[\left(\frac{z_a^2}{2}-\frac{h^2}{6}\right)h\nabla(\nabla\cdot\mathbf{u})+\left(z_a+\frac{h}{2}\right)h\nabla(\nabla\cdot h\mathbf{u})\right]$$

$$\psi_{\mathbf{M}} = \begin{bmatrix}\psi_{M_x}\\ \psi_{M_y}\end{bmatrix} = H_t\frac{z_a^2}{2}\nabla(\nabla\cdot\mathbf{u})+H_t z_a\nabla(\nabla\cdot h\mathbf{u})$$

$R_b = [R_{b_x},\ R_{b_y}]^{\mathrm{T}}$ = parametrization of wave breaking characteristics where:

$$R_{b_x} = \nabla\cdot\tilde{\mathbf{R}}_{b_x},\ \text{where } \tilde{\mathbf{R}}_{b_x} = \left[\nu(Hu)_x \quad \frac{\nu}{2}((Hu)_y+(Hv)_x)\right]^{\mathrm{T}} \text{ and}$$

$$R_{b_y} = \nabla\cdot\tilde{\mathbf{R}}_{b_y},\ \text{where } \tilde{\mathbf{R}}_{b_y} = \left[\frac{\nu}{2}((Hu)_y+(Hv)_x) \quad \nu(Hv)_y\right]^{\mathrm{T}}.$$

where $\nu = B\delta_b^2 H\eta_t$ is the eddy viscosity coefficient with $0 < B < 1$ and δ_b is a mixing length coefficient.

Numerical Model: Spatial discretization

- Advective (nonlinear) part and topography source term: Well-balanced FV formulation.
- Roe's approximate Riemann solver is used (Roe, 1981).
- Upwinding of the topography source term (Bermudez et al., 1994).
- High-order spatial accuracy: third-order **MUSCL**-type scheme (Barth, 1993).
- Satisfy the C-property (flow at rest) to higher spatial order: Addition of an extra term to bed upwinding (Hubbard and Garcia-Navarro, 2000 and Delis and Nikolos, 2009).
- Special treatment of **wet/dry fronts**.
- Dispersion terms: consistent FV approximations based on gradient and divergence computations (Kazolea et al., 2012) .

Numerical Model: Spatial discretization

- Advective (nonlinear) part and topography source term: Well-balanced FV formulation.
- Roe's approximate Riemann solver is used (Roe, 1981).
- Upwinding of the topography source term (Bermudez et al., 1994).
- High-order spatial accuracy: third-order **MUSCL**-type scheme (Barth, 1993).
- Satisfy the *C*-property (flow at rest) to higher spatial order: Addition of an extra term to bed upwinding (Hubbard and Garcia-Navarro, 2000 and Delis and Nikolos, 2009).
- Special treatment of **wet/dry fronts**.
- Dispersion terms: consistent FV approximations based on gradient and divergence computations (Kazolea et al., 2012) .

Numerical Model: Spatial discretization

- Advective (nonlinear) part and topography source term: Well-balanced FV formulation.
- Roe's approximate Riemann solver is used (Roe, 1981).
- Upwinding of the topography source term (Bermudez et al., 1994).
- High-order spatial accuracy: third-order **MUSCL**-type scheme (Barth, 1993).
- Satisfy the C-property (flow at rest) to higher spatial order: Addition of an extra term to bed upwinding (Hubbard and Garcia-Navarro, 2000 and Delis and Nikolos, 2009).
- Special treatment of **wet/dry fronts**.
- Dispersion terms: consistent FV approximations based on gradient and divergence computations (Kazolea et al., 2012) .

Numerical Model: Spatial discretization

- Advective (nonlinear) part and topography source term: Well-balanced FV formulation.
- Roe's approximate Riemann solver is used (Roe, 1981).
- Upwinding of the topography source term (Bermudez et al., 1994).
- High-order spatial accuracy: third-order **MUSCL**-type scheme (Barth, 1993).
- Satisfy the *C*-property (flow at rest) to higher spatial order: Addition of an extra term to bed upwinding (Hubbard and Garcia-Navarro, 2000 and Delis and Nikolos, 2009).
- Special treatment of **wet/dry fronts**.
- Dispersion terms: consistent FV approximations based on gradient and divergence computations (Kazolea et al., 2012) .

Numerical Model: Spatial discretization

- Advective (nonlinear) part and topography source term: Well-balanced FV formulation.
- Roe's approximate Riemann solver is used (Roe, 1981).
- Upwinding of the topography source term (Bermudez et al., 1994).
- High-order spatial accuracy: third-order **MUSCL**-type scheme (Barth, 1993).
- Satisfy the *C*-property (flow at rest) to higher spatial order: Addition of an extra term to bed upwinding (Hubbard and Garcia-Navarro, 2000 and Delis and Nikolos, 2009).
- Special treatment of **wet/dry fronts**.
- Dispersion terms: consistent FV approximations based on gradient and divergence computations (Kazolea et al., 2012) .

Numerical Model: Spatial discretization

- Advective (nonlinear) part and topography source term: Well-balanced FV formulation.
- Roe's approximate Riemann solver is used (Roe, 1981).
- Upwinding of the topography source term (Bermudez et al., 1994).
- High-order spatial accuracy: third-order **MUSCL**-type scheme (Barth, 1993).
- Satisfy the *C*-property (flow at rest) to higher spatial order: Addition of an extra term to bed upwinding (Hubbard and Garcia-Navarro, 2000 and Delis and Nikolos, 2009).
- Special treatment of **wet/dry fronts**.
- Dispersion terms: consistent FV approximations based on gradient and divergence computations (Kazolea et al., 2012) .

Numerical Model: Spatial discretization

- Advective (nonlinear) part and topography source term: Well-balanced FV formulation.
- Roe's approximate Riemann solver is used (Roe, 1981).
- Upwinding of the topography source term (Bermudez et al., 1994).
- High-order spatial accuracy: third-order **MUSCL**-type scheme (Barth, 1993).
- Satisfy the *C*-property (flow at rest) to higher spatial order: Addition of an extra term to bed upwinding (Hubbard and Garcia-Navarro, 2000 and Delis and Nikolos, 2009).
- Special treatment of **wet/dry fronts**.
- Dispersion terms: consistent FV approximations based on gradient and divergence computations (Kazolea et al., 2012) .

Discretization of the dispersive terms (mass equation)

Integral averaging:

$$(\psi_c)_P = \frac{1}{|C_P|}\iint_{C_P} \nabla\cdot\left[\left(\frac{z_a^2}{2}-\frac{h^2}{6}\right)h\nabla(\nabla\cdot\mathbf{u}) + \left(z_a+\frac{h}{2}\right)h\nabla(\nabla\cdot h\mathbf{u})\right]d\Omega$$

$$= \frac{1}{|C_P|}\sum_{Q\in K_P}\left\{\int_{\partial C_{PQ}}\left[\left(\frac{z_a^2}{2}-\frac{h^2}{6}\right)h\nabla(\nabla\cdot\mathbf{u})\right]\cdot\tilde{\mathbf{n}}dl + \int_{\partial C_{PQ}}\left[\left(z_a+\frac{h}{2}\right)h\nabla(\nabla\cdot h\mathbf{u})\right]\cdot\tilde{\mathbf{n}}dl\right\}$$

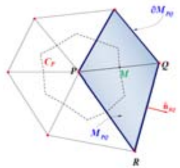

$$\int_{\partial C_{PQ}}\left(\frac{z_a^2}{2}-\frac{h^2}{6}\right)h\nabla(\nabla\cdot\mathbf{u})\cdot\tilde{\mathbf{n}}dl \approx \left[\left(\frac{z_a^2}{2}-\frac{h^2}{6}\right)h\right]_M[\nabla(\nabla\cdot\mathbf{u})\cdot\mathbf{n}_{PQ}]_M\,,$$

$$\int_{\partial C_{PQ}}\left(z_a+\frac{h}{2}\right)h\nabla(\nabla\cdot h\mathbf{u})\cdot\tilde{\mathbf{n}}dl \approx \left[\left(z_a+\frac{h}{2}\right)h\right]_M[\nabla(\nabla\cdot h\mathbf{u})\cdot\mathbf{n}_{PQ}]_M$$

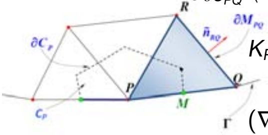

$$K_{PQ} := \{R\in\mathbb{N}\mid R \text{ is a vertex of } M_{PQ} \text{ and } RQ\in\partial M_{PQ}\}$$

$$(\nabla w)_M = \frac{1}{|M_{PQ}|}\sum_{\substack{R,Q\in K_{PQ}\\ R\neq Q}}\frac{1}{2}(w_R+w_Q)\,\mathbf{n}_{RQ}$$

Discretization of the dispersive terms (momentum equations)

$$\frac{1}{|C_P|}\iint_{C_P}\left(-\mathbf{u}\psi_c+\psi_{\mathbf{M}}\right)d\Omega=-\frac{\mathbf{u}_P}{|C_P|}\iint_{C_P}\psi_c d\Omega+\frac{1}{|C_P|}\iint_{C_P}\psi_{\mathbf{M}}d\Omega.$$

The ψ_c is discretized as before and the second term takes the discrete form:

$$\begin{aligned}(\psi_{\mathbf{M}})_P &= \frac{1}{|C_P|}\iint_{C_P}\psi_{\mathbf{M}}d\Omega=\frac{1}{|C_P|}\iint_{C_P}H_t\frac{z_a^2}{2}\nabla(\nabla\cdot\mathbf{u})+H_t z_a\nabla(\nabla\cdot h\mathbf{u})d\Omega\\ &= \frac{1}{|C_P|}\iint_{C_P}H_t\frac{z_a^2}{2}\nabla(\nabla\cdot\mathbf{u})d\Omega+\frac{1}{|C_P|}\iint_{C_P}H_t z_a\nabla(\nabla\cdot h\mathbf{u})d\Omega\\ &\approx \left[H_t\frac{z_a^2}{2}\right]_P\left[\nabla(\nabla\cdot\mathbf{u})\right]_P+\left[H_t z_a\right]_P\left[\nabla(\nabla\cdot h\mathbf{u})\right]_P,\end{aligned}$$

Time integration

Consider the semi-discrete scheme:

$$\frac{\partial \mathbf{U}_P}{\partial t} = \mathcal{L}(\mathbf{U})$$

Time Integration (match the order of truncation errors from dispersion terms):
Use 3rd order explicit Strong Stability-Preserving Runge-Kutta (SSP-RK):

$$\begin{aligned}
\mathbf{U}_P^{(1)} &= \mathbf{U}_P^{(n)} + \Delta t^n \mathcal{L}\left(\mathbf{U}^{(n)}\right); \\
\mathbf{U}_P^{(2)} &= \frac{3}{4}\mathbf{U}_P^{(n)} + \frac{1}{4}\mathbf{U}_P^{(1)} + \Delta t^n \frac{1}{4}\mathcal{L}\left(\mathbf{U}^{(1)}\right); \\
\mathbf{U}_P^{(n+1)} &= \frac{1}{3}\mathbf{U}_P^{(n)} + \frac{2}{3}\mathbf{U}_P^{(2)} + \Delta t^n \frac{2}{3}\mathcal{L}\left(\mathbf{U}^{(2)}\right)
\end{aligned}$$

Time step Δt^n estimated by a CFL stability condition as

$$\Delta t^n = CFL \cdot \min_P \left(\frac{R_P}{\left(\sqrt{u^2 + v^2} + c\right)_P^n} \right)$$

Velocity field recovery

From new solution variables $\mathbf{P} = [P_1, P_2]^{\mathrm{T}}$
At each step in the RK scheme a linear system $\mathbf{MV} = \mathbf{C}$ with $\mathbf{M} \in \mathbb{R}^{2N \times 2N}$ and $\mathbf{C} = [\mathbf{P}_1 \ \mathbf{P}_2 \cdots \ \mathbf{P}_N]^{\mathrm{T}}$, has to be solved to obtain the velocities $\mathbf{V} = [\mathbf{u}_1 \ \mathbf{u}_2 \ \cdots \ \mathbf{u}_N]^{\mathrm{T}}$. Each two rows of the system read as

$$H_P^{(i)} \left[\frac{z_a^2}{2} \nabla(\nabla \cdot \mathbf{u}) + z_a \nabla(\nabla \cdot h\mathbf{u}) + \mathbf{u} \right]_P^{(i)} = \mathbf{P}_P^{(i)}, \quad i = 1, 2, n+1.$$

Velocity field recovery

From new solution variables $\mathbf{P} = [P_1, P_2]^{\mathrm{T}}$
At each step in the RK scheme a linear system $\mathbf{MV} = \mathbf{C}$ with $\mathbf{M} \in \mathbb{R}^{2N\times 2N}$ and $\mathbf{C} = [\mathbf{P}_1 \ \mathbf{P}_2 \cdots \ \mathbf{P}_N]^{\mathrm{T}}$, has to be solved to obtain the velocities $\mathbf{V} = [\mathbf{u}_1 \ \mathbf{u}_2 \ \cdots \ \mathbf{u}_N]^{\mathrm{T}}$. Each two rows of the system read as

$$H_P^{(i)} \left[\frac{z_a^2}{2} \nabla(\nabla \cdot \mathbf{u}) + z_a \nabla(\nabla \cdot h\mathbf{u}) + \mathbf{u} \right]_P^{(i)} = \mathbf{P}_P^{(i)}, \quad i = 1, 2, n+1.$$

Important to (a) keep the unknown information needed at the minimum possible level (i.e neighboring nodes) and (b) exploit already computed geometrical information.

$$H_P \left[\frac{(z_a^2)_P}{2} \frac{1}{|C_P|} \sum_{Q \in K_P} (\nabla \cdot \mathbf{u})_M \mathbf{n}_{PQ} + \frac{(z_a)_P}{|C_P|} \sum_{Q \in K_P} (\nabla \cdot h\mathbf{u})_M \mathbf{n}_{PQ} + \mathbf{u}_P \right] = \mathbf{P}_P$$

Velocity field recovery

From new solution variables $\mathbf{P} = [P_1, P_2]^{\mathrm{T}}$
At each step in the RK scheme a linear system $\mathbf{MV} = \mathbf{C}$ with $\mathbf{M} \in \mathbb{R}^{2N\times 2N}$ and $\mathbf{C} = [\mathbf{P}_1\ \mathbf{P}_2 \cdots\ \mathbf{P}_N]^{\mathrm{T}}$, has to be solved to obtain the velocities $\mathbf{V} = [\mathbf{u}_1\ \mathbf{u}_2\ \cdots\ \mathbf{u}_N]^{\mathrm{T}}$. Each two rows of the system read as

$$H_P^{(i)}\left[\frac{z_a^2}{2}\nabla(\nabla\cdot\mathbf{u}) + z_a\nabla(\nabla\cdot h\mathbf{u}) + \mathbf{u}\right]_P^{(i)} = \mathbf{P}_P^{(i)}, \quad i = 1, 2, n+1.$$

Important to (a) keep the unknown information needed at the minimum possible level (i.e neighboring nodes) and (b) exploit already computed geometrical information.

$$H_P\left[\frac{(z_a^2)_P}{2}\frac{1}{|C_P|}\sum_{Q\in K_P}(\nabla\cdot\mathbf{u})_M\mathbf{n}_{PQ} + \frac{(z_a)_P}{|C_P|}\sum_{Q\in K_P}(\nabla\cdot h\mathbf{u})_M\mathbf{n}_{PQ} + \mathbf{u}_P\right] = \mathbf{P}_P$$

$$\frac{(z_a^2)_P}{2|C_P|}\sum_{Q\in K_P}\mathbf{A}_Q\mathbf{u}_Q + \mathbf{A}_P\mathbf{u}_P + \frac{(z_a)_P}{|C_P|}\sum_{Q\in K_P}\mathbf{B}_Q\mathbf{u}_Q + \mathbf{B}_P\mathbf{u}_P + \mathbf{I}\mathbf{u}_P = \frac{1}{H_P}\mathbf{P}_P,\ \ P = 1\ldots N$$

Solution of the linear system

- The matrix **M** is **sparse and structurally symmetric** but is also mesh dependent.

Solution of the linear system

- The matrix **M** is **sparse and structurally symmetric** but is also mesh dependent.
- Matrix **M** is stored in the **compressed sparse row (CSR)** format.

Solution of the linear system

- The matrix **M** is **sparse and structurally symmetric** but is also mesh dependent.
- Matrix **M** is stored in the **compressed sparse row (CSR)** format.
- The **ILUT preconditioner** from SPARSKIT package is used.

Solution of the linear system

- The matrix **M** is **sparse and structurally symmetric** but is also mesh dependent.
- Matrix **M** is stored in the **compressed sparse row (CSR)** format.
- The **ILUT preconditioner** from SPARSKIT package is used.
- The **reverse Cuthill–McKee (RCM)** algorithm is also employed to reorder the matrix elements as to minimize the matrix bandwidth.

Solution of the linear system

- The matrix **M** is **sparse and structurally symmetric** but is also mesh dependent.
- Matrix **M** is stored in the **compressed sparse row (CSR)** format.
- The **ILUT preconditioner** from SPARSKIT package is used.
- The **reverse Cuthill–McKee (RCM)** algorithm is also employed to reorder the matrix elements as to minimize the matrix bandwidth.
- System is solved using **Bi-Conjugate Gradient Stabilized** method (BiCGStab), with tolerance $5 \cdot 10^{-6}$

Solution of the linear system

- The matrix **M** is **sparse and structurally symmetric** but is also mesh dependent.
- Matrix **M** is stored in the **compressed sparse row (CSR)** format.
- The **ILUT preconditioner** from SPARSKIT package is used.
- The **reverse Cuthill–McKee (RCM)** algorithm is also employed to reorder the matrix elements as to minimize the matrix bandwidth.
- System is solved using **Bi-Conjugate Gradient Stabilized** method (BiCGStab), with tolerance $5 \cdot 10^{-6}$
- Convergence to the solution was obtained in one or two steps with the numerical solution for the velocities at the previous time step given as initial guess.

Boundary conditions and the internal source function

- **Wall (reflective) boundary condition:** $\mathbf{u} \cdot \widetilde{\mathbf{n}} = 0$ for $\mathbf{x} \in \partial\Omega$
  By conservation of mass (no loss or gain through the wall)

$$\frac{\partial}{\partial t} \iint_{\Omega} H d\Omega + \int_{\partial\Omega} \left[H\mathbf{u} + \left(\frac{z_a^2}{2} - \frac{h^2}{6} \right) h\nabla(\nabla \cdot \mathbf{u}) + \left(z_a + \frac{h}{2} \right) h\nabla(\nabla \cdot h\mathbf{u}) \right] \cdot \widetilde{\mathbf{n}} dl = 0$$

Define the normal boundary advective flux in weak form,

$\mathbf{\Phi}_{P,\Gamma} = \begin{bmatrix} 0 \\ \frac{1}{2} g (H^\star)^2 n_{P,1x} \\ \frac{1}{2} g (H^\star)^2 n_{P,1y} \end{bmatrix}$ by the **method of characteristics**

Boundary conditions and the internal source function

- **Wall (reflective) boundary condition:** $\mathbf{u}\cdot\widetilde{\mathbf{n}} = 0$ for $\mathbf{x} \in \partial\Omega$
  By conservation of mass (no loss or gain through the wall)

$$\frac{\partial}{\partial t}\iint_{\Omega} H d\Omega + \int_{\partial\Omega}\left[H\mathbf{u} + \left(\frac{z_a^2}{2} - \frac{h^2}{6}\right)h\nabla(\nabla\cdot\mathbf{u}) + \left(z_a + \frac{h}{2}\right)h\nabla(\nabla\cdot h\mathbf{u})\right]\cdot\widetilde{\mathbf{n}}dl = 0$$

  Define the normal boundary advective flux in weak form,

  $\mathbf{\Phi}_{P,\Gamma} = \begin{bmatrix} 0 \\ \frac{1}{2}g(H^\star)^2 n_{P,1x} \\ \frac{1}{2}g(H^\star)^2 n_{P,1y} \end{bmatrix}$ by the **method of characteristics**

- **Absorbing boundaries:** should dissipate the energy of incoming waves

  Sponge layer is defined: $m(\mathbf{x}) = \sqrt{1 - \left(\frac{\mathbf{x} - d(\mathbf{x})}{L_s}\right)^2}, \; L \le L_s \le 1.5L,$

Boundary conditions and the internal source function

- **Wall (reflective) boundary condition:** $\mathbf{u} \cdot \widetilde{\mathbf{n}} = 0$ for $\mathbf{x} \in \partial\Omega$
  By conservation of mass (no loss or gain through the wall)

$$\frac{\partial}{\partial t} \iint_{\Omega} H d\Omega + \int_{\partial\Omega} \left[H\mathbf{u} + \left(\frac{z_a^2}{2} - \frac{h^2}{6} \right) h\nabla(\nabla \cdot \mathbf{u}) + \left(z_a + \frac{h}{2} \right) h\nabla(\nabla \cdot h\mathbf{u}) \right] \cdot \widetilde{\mathbf{n}} dl = 0$$

  Define the normal boundary advective flux in weak form,

$$\mathbf{\Phi}_{P,\Gamma} = \begin{bmatrix} 0 \\ \frac{1}{2} g(H^\star)^2 n_{P,1x} \\ \frac{1}{2} g(H^\star)^2 n_{P,1y} \end{bmatrix}$$ by the **method of characteristics**

- **Absorbing boundaries:** should dissipate the energy of incoming waves

  Sponge layer is defined: $m(\mathbf{x}) = \sqrt{1 - \left(\frac{\mathbf{x} - d(\mathbf{x})}{L_s} \right)^2}$, $L \leq L_s \leq 1.5L$,

- **Internal source function** for regular waves (Wei et al., 1993) added to the mass equation

$$S(\mathbf{x}, t) = D^* \exp\left(\gamma (x - x_s)^2 \right) \sin(\lambda y - \omega t)$$

Wave breaking models

Eddy viscosity wave breaking model

$$
\begin{aligned}
(\mathbf{R_b})_P &= \frac{1}{|C_P|}\iint_{C_P} \mathbf{R_b}\, d\Omega = \frac{1}{|C_P|}\iint_{C_P}\begin{bmatrix} \nabla\cdot\tilde{\mathbf{R}}_{b_y} \\ \nabla\cdot\tilde{\mathbf{R}}_{b_x}\end{bmatrix} d\Omega \\
&= \frac{1}{|C_P|}\int_{\partial C_{PQ}}\begin{bmatrix} \tilde{\mathbf{R}}_{b_x}\cdot\widetilde{\mathbf{n}} \\ \tilde{\mathbf{R}}_{b_y}\cdot\widetilde{\mathbf{n}}\end{bmatrix} dl \approx \frac{1}{|C_P|}\begin{bmatrix} \tilde{\mathbf{R}}_{b_x}\cdot\mathbf{n}_{PQ} \\ \tilde{\mathbf{R}}_{b_y}\cdot\mathbf{n}_{PQ}\end{bmatrix}_M
\end{aligned}
$$

Wave breaking models

Eddy viscosity wave breaking model

$$
\begin{aligned}
(\mathbf{R_b})_P &= \frac{1}{|C_P|}\iint_{C_P}\mathbf{R_b}\,d\Omega = \frac{1}{|C_P|}\iint_{C_P}\begin{bmatrix}\nabla\cdot\tilde{\mathbf{R}}_{b_y}\\ \nabla\cdot\tilde{\mathbf{R}}_{b_x}\end{bmatrix}d\Omega \\
&= \frac{1}{|C_P|}\int_{\partial C_{PQ}}\begin{bmatrix}\tilde{\mathbf{R}}_{b_x}\cdot\widetilde{\mathbf{n}}\\ \tilde{\mathbf{R}}_{b_y}\cdot\widetilde{\mathbf{n}}\end{bmatrix}dl \approx \frac{1}{|C_P|}\begin{bmatrix}\tilde{\mathbf{R}}_{b_x}\cdot\mathbf{n}_{PQ}\\ \tilde{\mathbf{R}}_{b_y}\cdot\mathbf{n}_{PQ}\end{bmatrix}_M
\end{aligned}
$$

Hybrid models

- Hybrid(ϵ) $\rightarrow$ BT degenerate into NSWE as dispersive terms become negligible.
    - Criterion: $\epsilon = \frac{A}{h} \leq 0.8$
    - In post breaking region $\epsilon < 0.4$ in order to switch NSWE/BT.

Wave breaking models

Eddy viscosity wave breaking model

$$
\begin{aligned}
(\mathbf{R_b})_P &= \frac{1}{|C_P|}\iint_{C_P} \mathbf{R_b}\, d\Omega = \frac{1}{|C_P|}\iint_{C_P}\begin{bmatrix} \nabla\cdot\tilde{\mathbf{R}}_{b_y} \\ \nabla\cdot\tilde{\mathbf{R}}_{b_x}\end{bmatrix} d\Omega \\
&= \frac{1}{|C_P|}\int_{\partial C_{PQ}}\begin{bmatrix} \tilde{\mathbf{R}}_{b_x}\cdot\widetilde{\mathbf{n}} \\ \tilde{\mathbf{R}}_{b_y}\cdot\widetilde{\mathbf{n}}\end{bmatrix} dl \approx \frac{1}{|C_P|}\begin{bmatrix} \tilde{\mathbf{R}}_{b_x}\cdot\mathbf{n}_{PQ} \\ \tilde{\mathbf{R}}_{b_y}\cdot\mathbf{n}_{PQ}\end{bmatrix}_M
\end{aligned}
$$

Hybrid models

- Hybrid(ϵ) $\rightarrow$ BT degenerate into NSWE as dispersive terms become negligible.
  - Criterion: $\epsilon = \frac{A}{h} \leq 0.8$
  - In post breaking region $\epsilon < 0.4$ in order to switch NSWE/BT.
- New Hybrid
  - criteria: $\eta_t \geq \gamma\sqrt{gh},\ \gamma \in [0.35,\ 0.65],\ \|\eta_x\| \geq tan(\phi_c)$.
  - Distinguish the different breaking waves.
  - Find non-breaking undular bores checking the Froude number.
  - Extend the computational region of the NSWE.

Suppression of the dispersive terms

- Not clear how the **switching** between the two models is implemented

Suppression of the dispersive terms

- Not clear how the **switching** between the two models is implemented
- **Discontinuity** at the switching point BT/NSWE, causing spurious **oscillations**.

Suppression of the dispersive terms

- Not clear how the **switching** between the two models is implemented
- **Discontinuity** at the switching point BT/NSWE, causing spurious **oscillations**.
- Matrix **M** can not be change.

Suppression of the dispersive terms

- Not clear how the **switching** between the two models is implemented
- **Discontinuity** at the switching point BT/NSWE, causing spurious **oscillations**.
- Matrix **M** can not be change.
- Need of a ”**clever**” **implementation**.

Suppression of the dispersive terms

- Not clear how the **switching** between the two models is implemented
- **Discontinuity** at the switching point BT/NSWE, causing spurious **oscillations**.
- Matrix **M** can not be change.
- Need of a "**clever**" **implementation**.

Methodology

0. Starting with the solution vector $\mathbf{U}_P^n, P = 1, \ldots, N$, at time t^n,
1. $\mathbf{H}$ is computed $\forall C_P$ using the BT model (named from now on $\mathbf{H}_{BT}^{n+1}$).
   1.1 If breaking is on for $N_{br} < N$ cells $\Rightarrow$ additional solution vector $\mathbf{H}_{BT}^{n+1} - \psi_c$ named $\mathbf{H}_{BT/SW}^{n+1}$.
2. $\mathbf{P}_{BT}^{n+1}$ is computed $\forall C_P$ / $\partial_t \mathbf{H}^{n+1} \approx \dfrac{\mathbf{H}_{BT}^{n+1} - \mathbf{H}^n}{\Delta t^{n+1}}$ for the $\psi_{\mathbf{M}}$.
   2.1 N_{br} cells $\Rightarrow \mathbf{P}_{BT/SW}^{n+1} \rightarrow \mathbf{P}_{BT}^{n+1} - \psi_c - \psi_{\mathbf{M}} \Rightarrow [(Hu),\ (Hv)]^{n+1,\mathrm{T}}$
3. $\mathbf{MV} = \mathbf{C}$,with $\mathbf{C} = [\mathbf{P}_1^{n+1}, \mathbf{P}_2^{n+1}, \cdots, \mathbf{P}_N^{n+1}]_{BT}^{\mathrm{T}} \rightarrow \mathbf{u}_{BT}^{n+1}$
4. Final solution: $\mathbf{H}_{BT/SW}^{n+1},\ \mathbf{P}_{BT/SW}^{n+1},\ \mathbf{u}_{BT/SW}^{n+1} \rightarrow \mathbf{u}_{BT}^{n+1}$ vector with its values at the breaking nodes replaced by those of $\mathbf{u}_{SW}^{n+1}$.

Numerical Results: Spatial accuracy

- Solitary wave: $A/h = 0.1,\ (x,y) \in [0,\ 300] \times [0, 5m]$
- Reference solution of $N = 232,849$ nodes

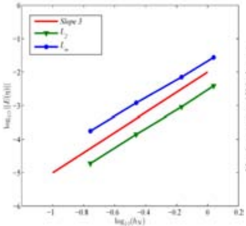

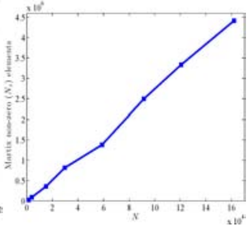

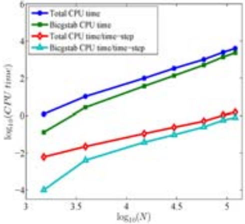

Solitary wave interaction with a vertical circular cylinder

Area: $(x, y) = [-4, 10m] \times [0, 0.55m]$, $A/h = 0.25$, $N = 10,609$

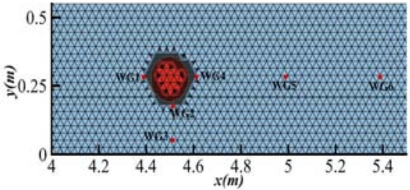

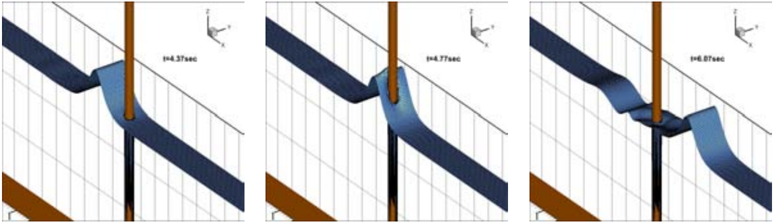

Solitary wave interaction with a vertical circular cylinder

Wave Gauges:

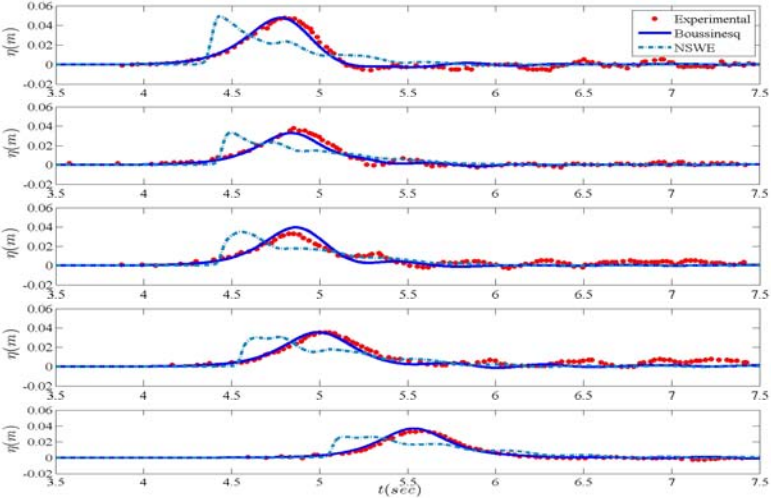

Run-up of a solitary wave on a conical island (Briggs et al. 1995)

Area: $(x, y) = [-5, 28m] \times [0, 30m]$, $A/h = 0.18$, $N = 52,191$, $CFL = 0.8$
Using mesh $h-$ enrichment

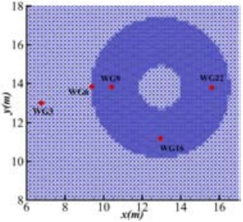

Run-up of a solitary wave on a conical island (Briggs et al. 1995)

Area: $(x, y) = [-5, 28m] \times [0, 30m]$, $A/h = 0.18$, $N = 52,191$, $CFL = 0.8$
Using mesh $h-$ enrichment

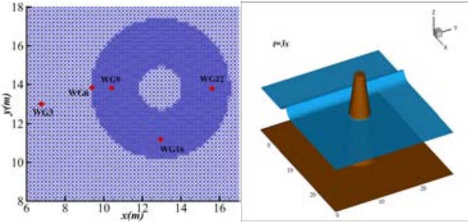

Run-up of a solitary wave on a conical island (Briggs et al. 1995)

Area: $(x, y) = [-5, 28m] \times [0, 30m]$, $A/h = 0.18$, $N = 52,191$, $CFL = 0.8$
Using mesh $h-$ enrichment

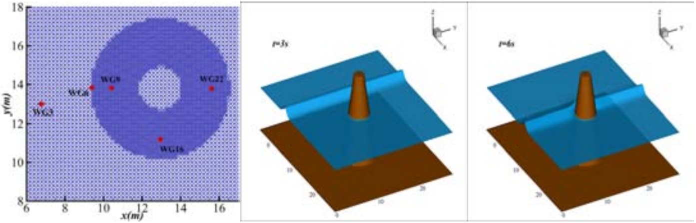

Run-up of a solitary wave on a conical island (Briggs et al. 1995)

Area: $(x, y) = [-5, 28m] \times [0, 30m]$, $A/h = 0.18$, $N = 52,191$, $CFL = 0.8$
Using mesh $h-$ enrichment

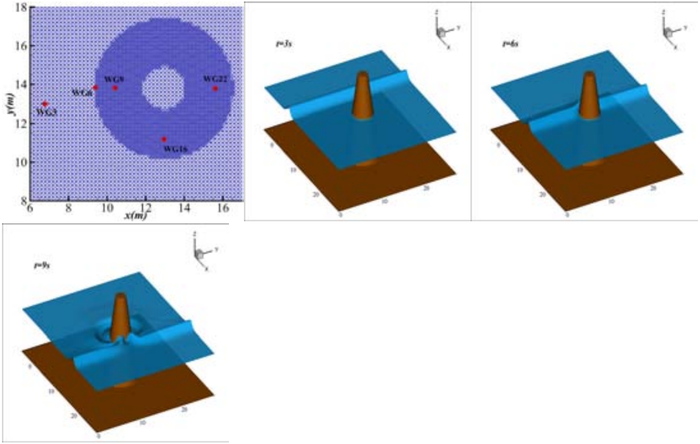

Run-up of a solitary wave on a conical island (Briggs et al. 1995)

Area: $(x, y) = [-5, 28m] \times [0, 30m]$, $A/h = 0.18$, $N = 52,191$, $CFL = 0.8$
Using mesh $h-$ enrichment

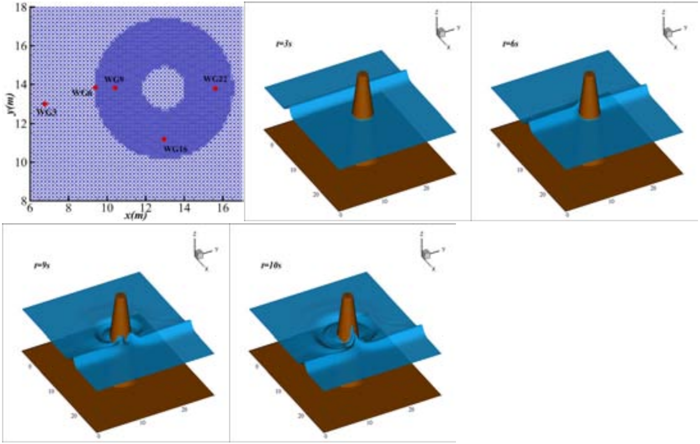

Run-up of a solitary wave on a conical island (Briggs et al. 1995)

Area: $(x, y) = [-5, 28m] \times [0, 30m]$, $A/h = 0.18$, $N = 52,191$, $CFL = 0.8$
Using mesh $h-$ enrichment

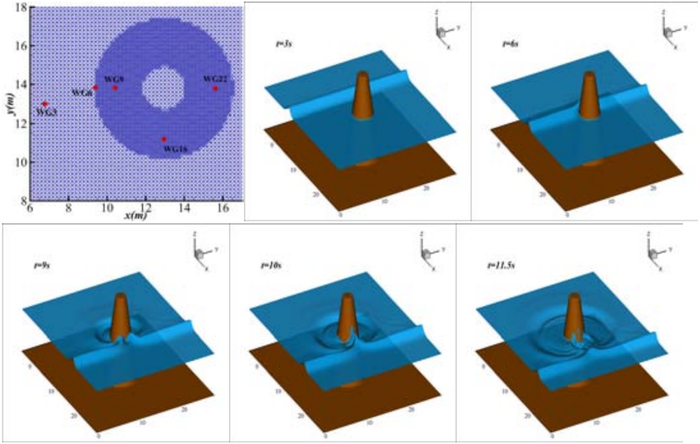

Run-up of a solitary wave on a conical island (Briggs et al. 1995)

Area: $(x, y) = [-5, 28m] \times [0, 30m]$, $A/h = 0.18$, $N = 52,191$, $CFL = 0.8$
Using mesh $h-$ enrichment

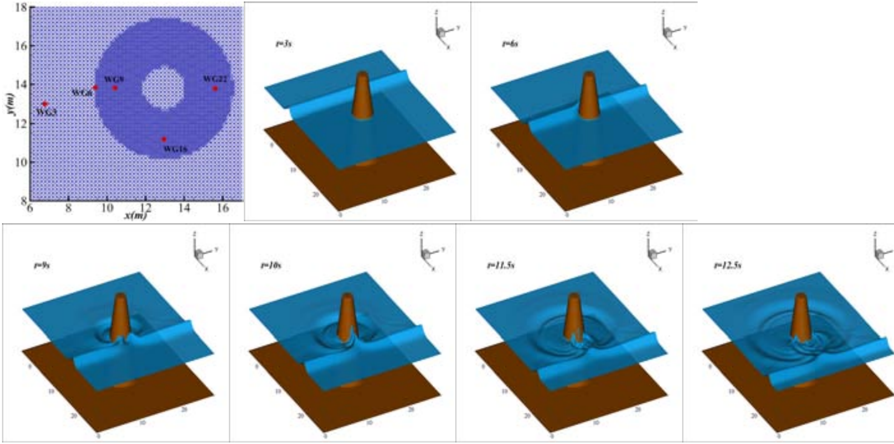

Run-up of a solitary wave on a conical island (cont)

Time series of surface elevation at wave gauges around the island:

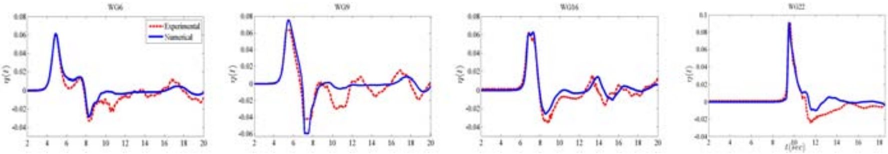

Run-up of a solitary wave on a conical island (cont)

Time series of surface elevation at wave gauges around the island:

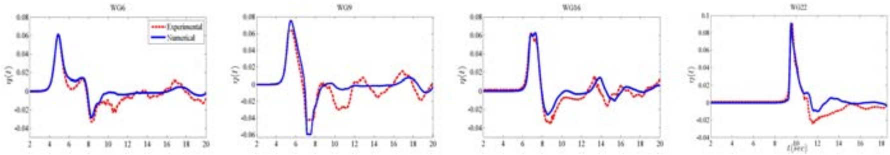

Experimental measurements and numerical runup around the island:

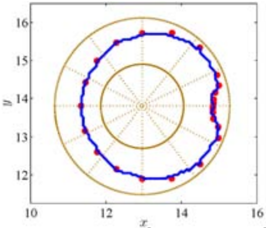

Simulation ∼ 28min on a single 2.4GHz Intel Core 2 Quad Q6600 processor

Wave propagation over a semicircular shoal (Whalin 1971)

$$T = 2.0s, \quad h/L = 0.117, \quad A/h = 0.0165, \quad kh = 0.735 \text{ and } S = 1.198$$

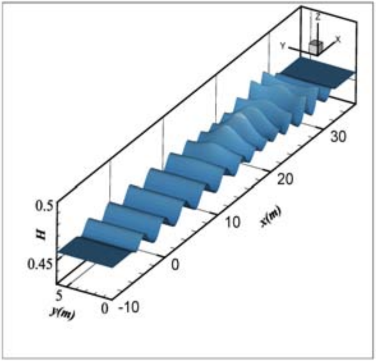

Wave propagation over a semicircular shoal (Whalin 1971)

$T = 2.0s, \quad h/L = 0.117, \quad A/h = 0.0165, \quad kh = 0.735$ and $S = 1.198$

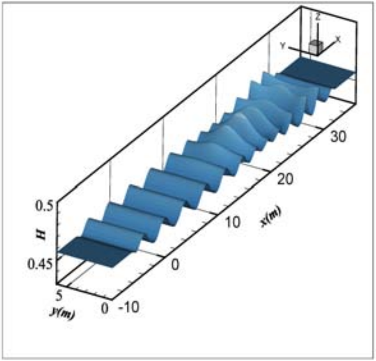

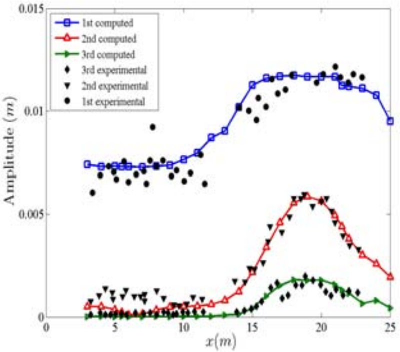

Free surface and spatial evolution of the 1st, 2nd and 3rd harmonic

Solitary wave run-up on a plane beach (Synolakis, 1987)

Area: $(x, y) = [-20, 60m] \times [0, 1m]$, $A/h = 0.28$, $N = 8,816$,
$CFL = 0.4$, $n_m = 0.01$

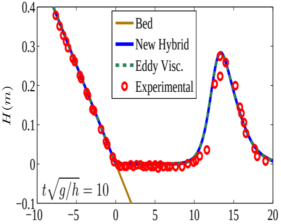

Solitary wave run-up on a plane beach (Synolakis, 1987)

Area: $(x, y) = [-20, 60m] \times [0, 1m]$, $A/h = 0.28$, $N = 8,816$,
$CFL = 0.4$, $n_m = 0.01$

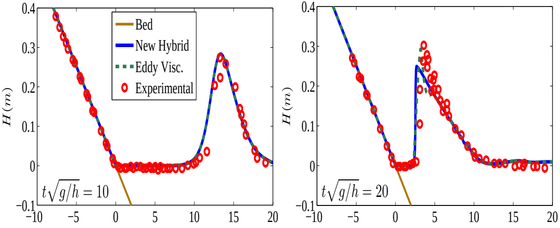

Solitary wave run-up on a plane beach (Synolakis, 1987)

Area: $(x, y) = [-20, 60m] \times [0, 1m]$, $A/h = 0.28$, $N = 8,816$,
$CFL = 0.4$, $n_m = 0.01$

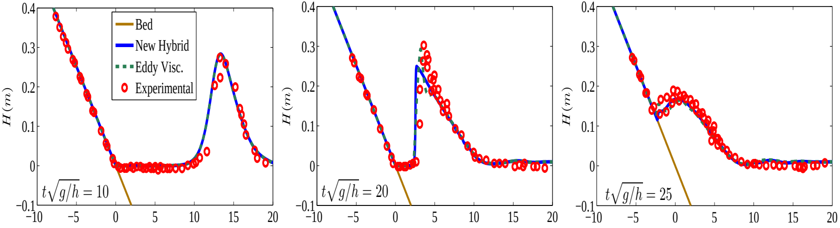

Solitary wave run-up on a plane beach (Synolakis, 1987)

Area: $(x, y) = [-20, 60m] \times [0, 1m]$, $A/h = 0.28$, $N = 8,816$,
$CFL = 0.4$, $n_m = 0.01$

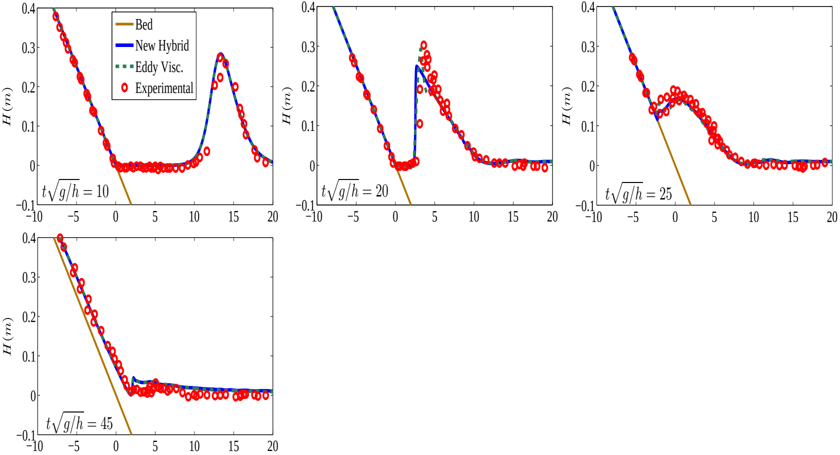

Solitary wave run-up on a plane beach (Synolakis, 1987)

Area: $(x, y) = [-20, 60m] \times [0, 1m]$, $A/h = 0.28$, $N = 8,816$, $CFL = 0.4$, $n_m = 0.01$

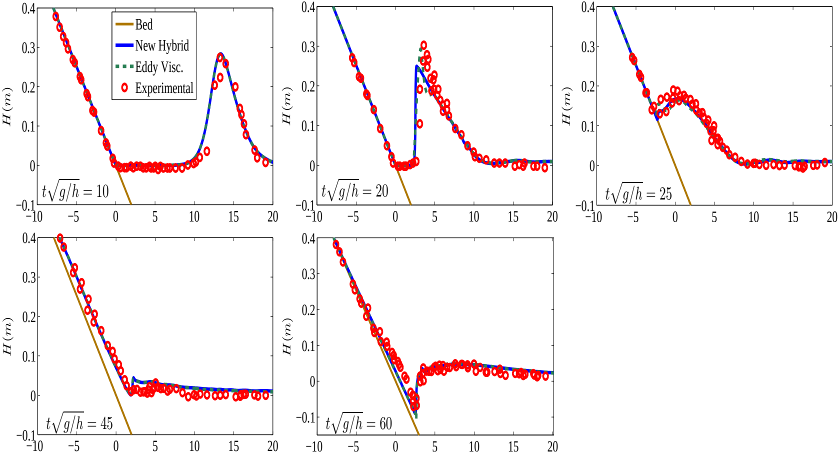

Solitary wave run-up on a plane beach (Synolakis, 1987)

Area: $(x, y) = [-20, 60m] \times [0, 1m]$, $A/h = 0.28$, $N = 8,816$,
$CFL = 0.4$, $n_m = 0.01$

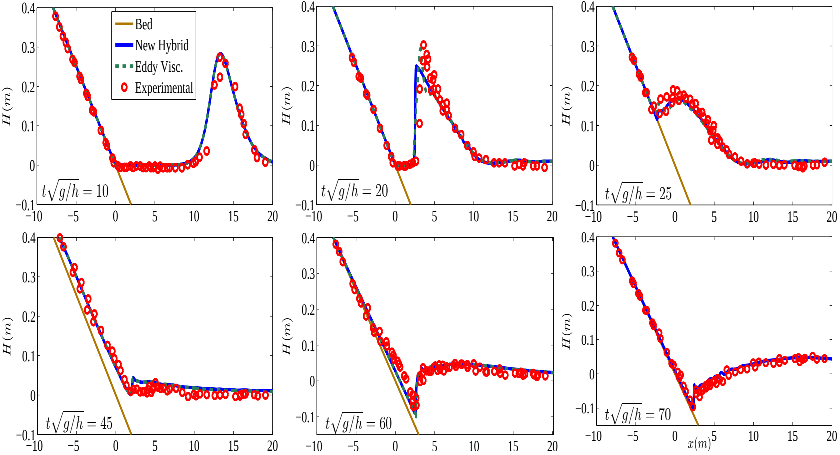

Wave over a bar (Beji and Battjes, 1993)

$$(x, y) = [-10, 30m] \times [0, 0.8m], \;\; H = 0.02m, \;\; T = 2.02s, \; N = 40,364$$

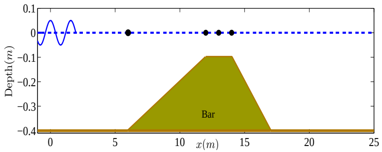

Wave over a bar (Beji and Battjes, 1993)

$$(x, y) = [-10, 30m] \times [0, 0.8m], \;\; H = 0.02m, \;\; T = 2.02s, \; N = 40,364$$

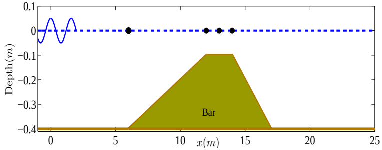

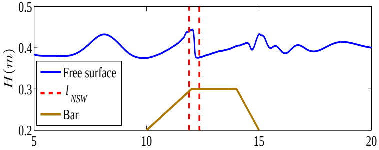

Wave over a bar (Beji and Battjes, 1993)

$$(x, y) = [-10, 30m] \times [0, 0.8m],\ \ H = 0.02m,\ \ T = 2.02s,\ N = 40,364$$

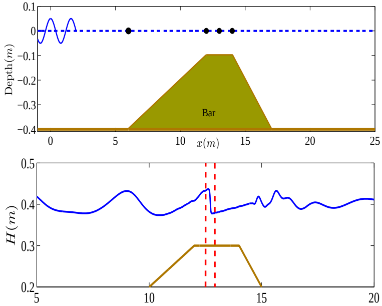

Wave over a bar (Beji and Battjes, 1993)

$$(x, y) = [-10, 30m] \times [0, 0.8m], \;\; H = 0.02m, \;\; T = 2.02s, \; N = 40,364$$

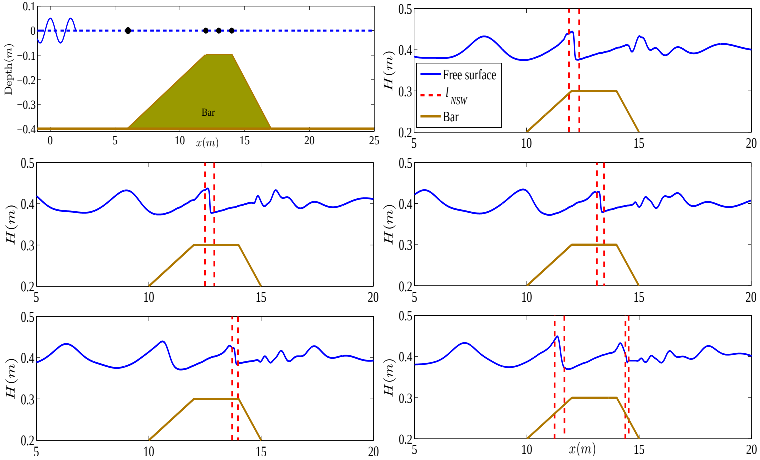

Wave over a bar (Beji and Battjes, 1993)

Wave gauges:

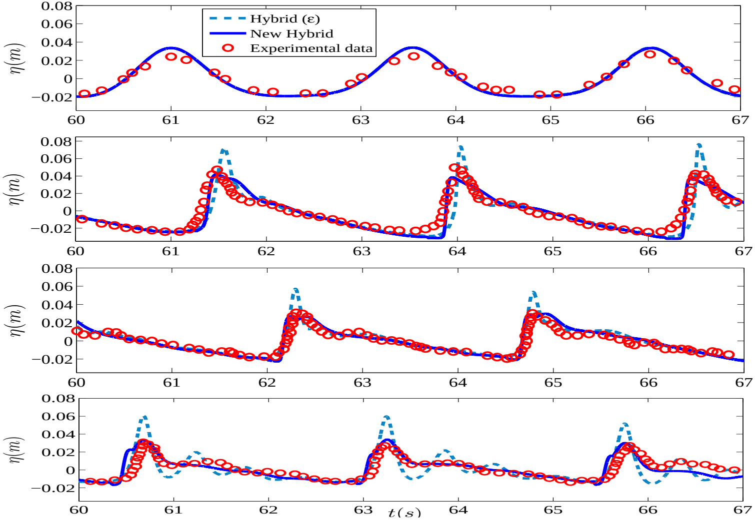

A two-dimensional reef (Roeber, 2009)

Area: $(x, y) = [0, 83m] \times [0, 1m]$, $A/h = 0.3$, $N = 10,900$, $n_m = 0.014$

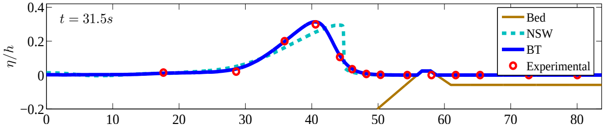

Shoaling

A two-dimensional reef(Roeber, 2009)

Area: $(x, y) = [0, 83m] \times [0, 1m]$, $A/h = 0.3$, $N = 10,900$, $n_m = 0.014$

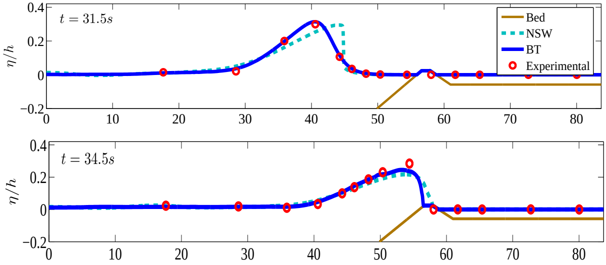

Shoaling

During breaking

A two-dimensional reef (Roeber, 2009)

Area: $(x, y) = [0, 83m] \times [0, 1m]$, $A/h = 0.3$, $N = 10,900$, $n_m = 0.014$

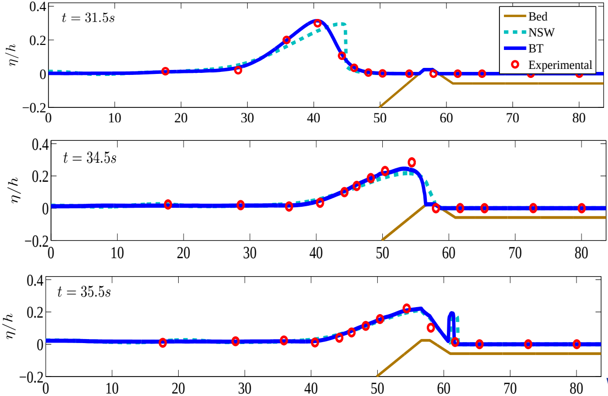

Shoaling

During breaking

Wave jet hits still water

A two-dimensional reef (Roeber, 2009)

Area: $(x, y) = [0, 83m] \times [0, 1m]$, $A/h = 0.3$, $N = 10,900$, $n_m = 0.014$

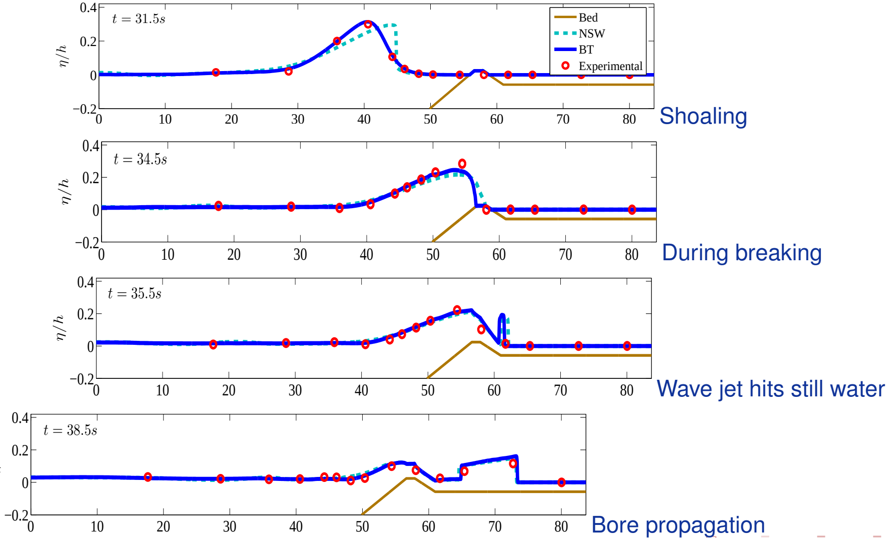

A two-dimensional reef(Roeber, 2009)

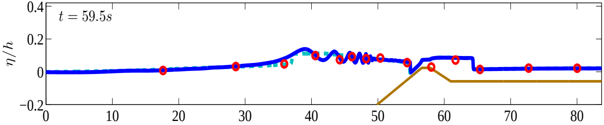

Hydraulic jump

A two-dimensional reef (Roeber, 2009)

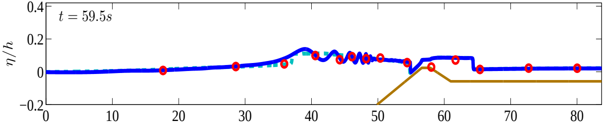

Hydraulic jump

Time series of surface elevation at wave gauges:

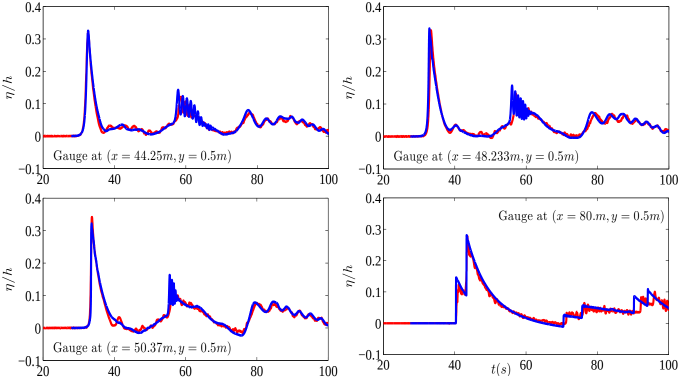

A two-dimensional reef (Roeber, 2009)

Spatial snapshots along the centerline:

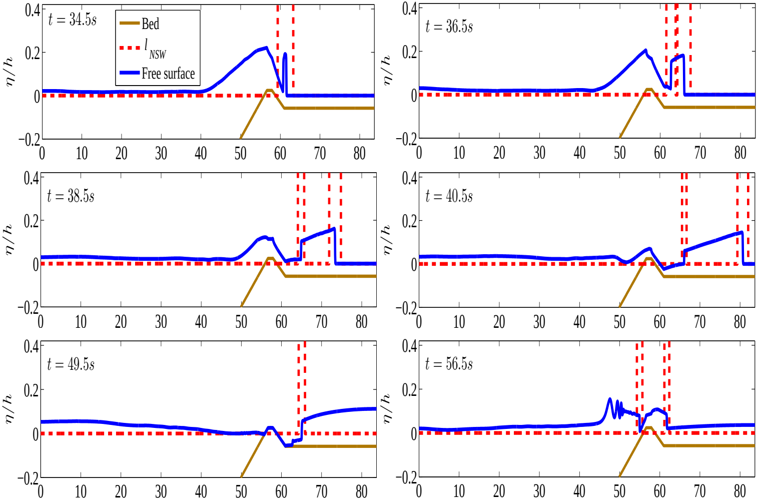

A three-dimensional reef (Lynett et al., 2009)

Area: $(x, y) = [0, 45m] \times [-13m, 13m]$, $A/h = 0.5$, $N = 87,961$

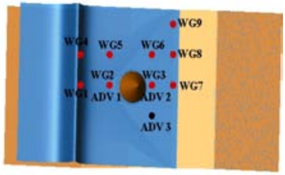

A three-dimensional reef(Lynett et al., 2009)

Area: $(x, y) = [0, 45m] \times [-13m, 13m]$, $A/h = 0.5$, $N = 87,961$

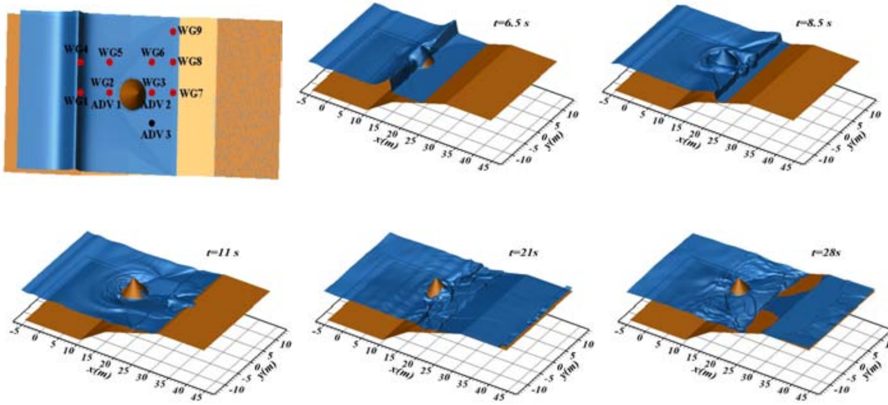

A three-dimensional reef (Lynett et al., 2009)

Time series of surface elevation at wave gauges:

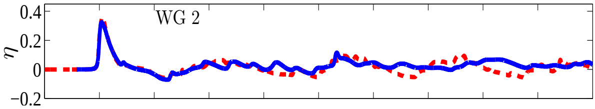

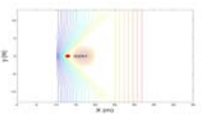

A three-dimensional reef (Lynett et al., 2009)

Time series of surface elevation at wave gauges:

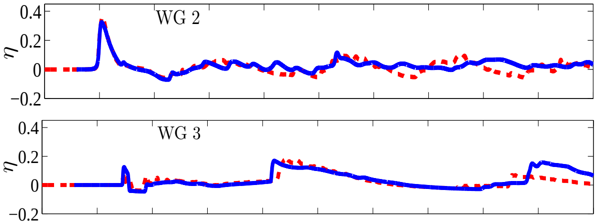

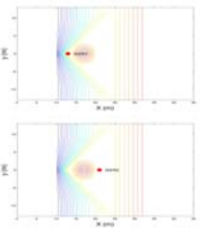

A three-dimensional reef (Lynett et al., 2009)

Time series of surface elevation at wave gauges:

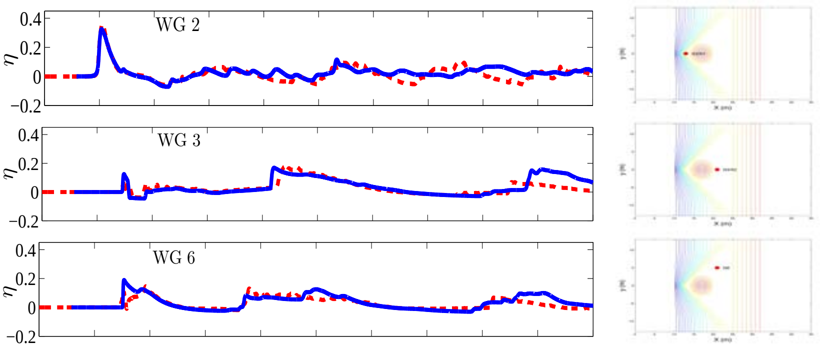

A three-dimensional reef (Lynett et al., 2009)

Time series of surface elevation at wave gauges:

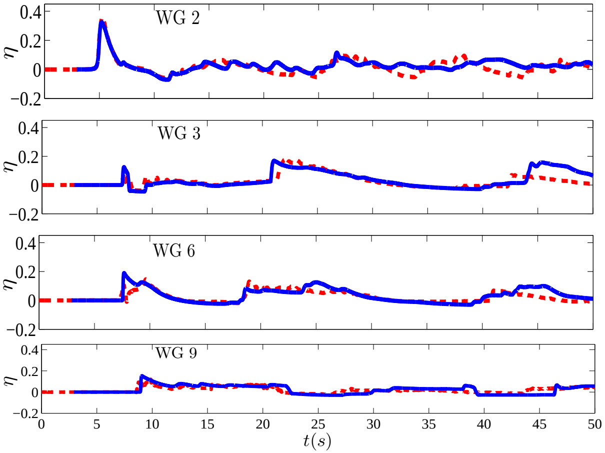

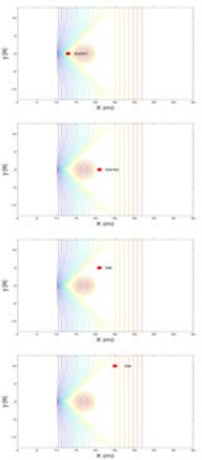

A three-dimensional reef (Lynett et al., 2009)

Time series of velocities at wave gauges:

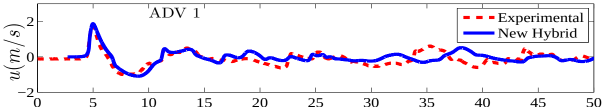

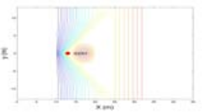

A three-dimensional reef(Lynett et al., 2009)

Time series of velocities at wave gauges:

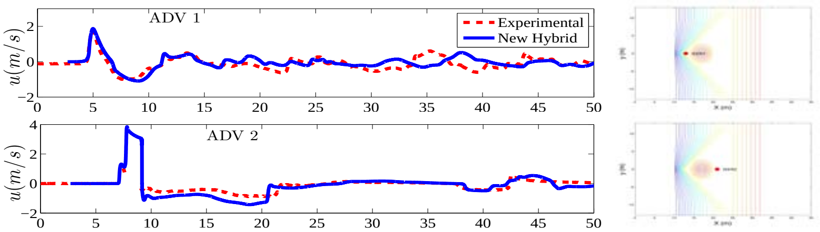

A three-dimensional reef (Lynett et al., 2009)

Time series of velocities at wave gauges:

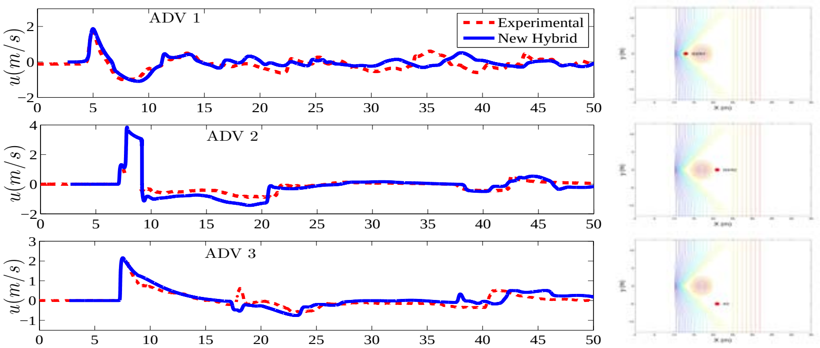

A three-dimensional reef (Lynett et al., 2009)

Time series of velocities at wave gauges:

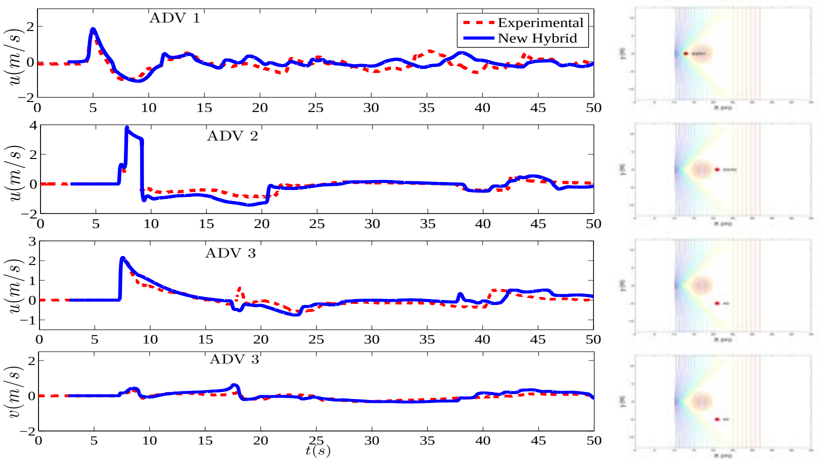

Conclusions

- A 2D unstructured FV scheme numerical model has been developed for solving Nwogu's extended BT equations formulated as to have **identical flux terms as to the NSWE**.

Conclusions

- A 2D unstructured FV scheme numerical model has been developed for solving Nwogu's extended BT equations formulated as to have **identical flux terms as to the NSWE**.
- **Conservative** formulation and **higher-order** FV scheme enhance the applicability of the model without altering its dispersion characteristics.

Conclusions

- A 2D unstructured FV scheme numerical model has been developed for solving Nwogu's extended BT equations formulated as to have **identical flux terms as to the NSWE**.
- **Conservative** formulation and **higher-order** FV scheme enhance the applicability of the model without altering its dispersion characteristics.
- The well-balanced topography and wet/dry front discretizations provided accurate conservative and stable wave propagation shoaling and run-up.

Conclusions

- A 2D unstructured FV scheme numerical model has been developed for solving Nwogu's extended BT equations formulated as to have **identical flux terms as to the NSWE**.
- **Conservative** formulation and **higher-order** FV scheme enhance the applicability of the model without altering its dispersion characteristics.
- The well-balanced topography and wet/dry front discretizations provided accurate conservative and stable wave propagation shoaling and run-up.
- The **edge-based structure** adopted can provide computational efficiency, since most of the geometric quantities needed can be calculated in a pre-processing stage.

Conclusions

- A 2D unstructured FV scheme numerical model has been developed for solving Nwogu's extended BT equations formulated as to have **identical flux terms as to the NSWE**.
- **Conservative** formulation and **higher-order** FV scheme enhance the applicability of the model without altering its dispersion characteristics.
- The well-balanced topography and wet/dry front discretizations provided accurate conservative and stable wave propagation shoaling and run-up.
- The **edge-based structure** adopted can provide computational efficiency, since most of the geometric quantities needed can be calculated in a pre-processing stage.
- Different type of **wave breaking** can be implemented. The **New Hybrid** model proved more stable and accurate than the others applied in this work.

Conclusions

- A 2D unstructured FV scheme numerical model has been developed for solving Nwogu's extended BT equations formulated as to have **identical flux terms as to the NSWE**.
- **Conservative** formulation and **higher-order** FV scheme enhance the applicability of the model without altering its dispersion characteristics.
- The well-balanced topography and wet/dry front discretizations provided accurate conservative and stable wave propagation shoaling and run-up.
- The **edge-based structure** adopted can provide computational efficiency, since most of the geometric quantities needed can be calculated in a pre-processing stage.
- Different type of **wave breaking** can be implemented. The **New Hybrid** model proved more stable and accurate than the others applied in this work.
- Relatively straight forward to **extend existing NSWE codes** that use (unstructured) FV schemes as to include dispersion characteristics for deeper water simulations.

Conclusions

- A 2D unstructured FV scheme numerical model has been developed for solving Nwogu's extended BT equations formulated as to have **identical flux terms as to the NSWE**.
- **Conservative** formulation and **higher-order** FV scheme enhance the applicability of the model without altering its dispersion characteristics.
- The well-balanced topography and wet/dry front discretizations provided accurate conservative and stable wave propagation shoaling and run-up.
- The **edge-based structure** adopted can provide computational efficiency, since most of the geometric quantities needed can be calculated in a pre-processing stage.
- Different type of **wave breaking** can be implemented. The **New Hybrid** model proved more stable and accurate than the others applied in this work.
- Relatively straight forward to **extend existing NSWE codes** that use (unstructured) FV schemes as to include dispersion characteristics for deeper water simulations.

References

1. A. I. Delis, M. Kazolea, and N. A Kampanis. A robust high resolution finite volume scheme for the simulation of long waves over complex domain. *Int. J. Num. Meth. Fluids*, 56:419, 2008.
2. A. I. Delis, I. A Nikolos, and M. Kazolea. Performance and comparison of cellcentered and node-centered unstructured finite volume discretizations for shallow water free surface flows. *Arch. Comput. Methods Eng.*, 18:57, 2011.
3. M. Kazolea and A. I. Delis. A well-balanced shock-capturing hybrid finite volume-finite difference numerical scheme for extended 1D Boussinesq models. *Applied Numerical Mathematics*, 67:167186, 2013.
4. M. Kazolea, A. I. Delis, I. A Nikolos, and C. E. Synolakis. An unstructured finite volume numerical scheme for extended 2D Boussinesq-type equations.*Coast. Eng.*, 69:4266, 2012.

Thank you for your attention!!

Solitary wave run-up on a plane beach

Area: $x \in [-20, 60m]$ $A/h = 0.04$, $Dx = 0.05$, $CFL = 0.4$, $n_m = 0.01$

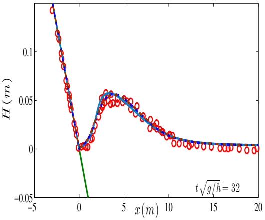

Solitary wave run-up on a plane beach

Area: $x \in [-20, 60m]$ $A/h = 0.04$, $Dx = 0.05$, $CFL = 0.4$, $n_m = 0.01$

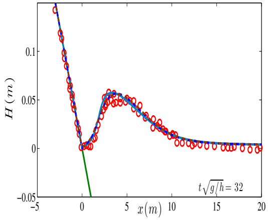

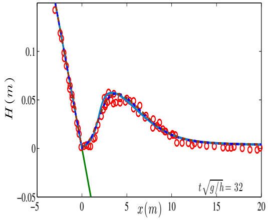

Solitary wave run-up on a plane beach

Area: $x \in [-20, 60m]$ $A/h = 0.04$, $Dx = 0.05$, $CFL = 0.4$, $n_m = 0.01$

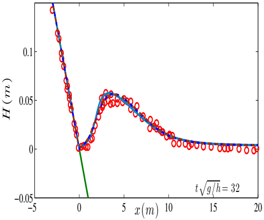

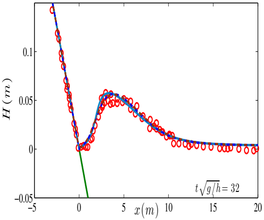

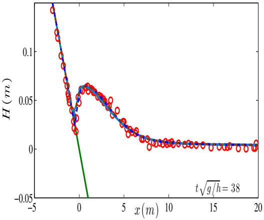

Solitary wave run-up on a plane beach

Area: $x \in [-20, 60m]$ $A/h = 0.04$, $Dx = 0.05$, $CFL = 0.4$, $n_m = 0.01$

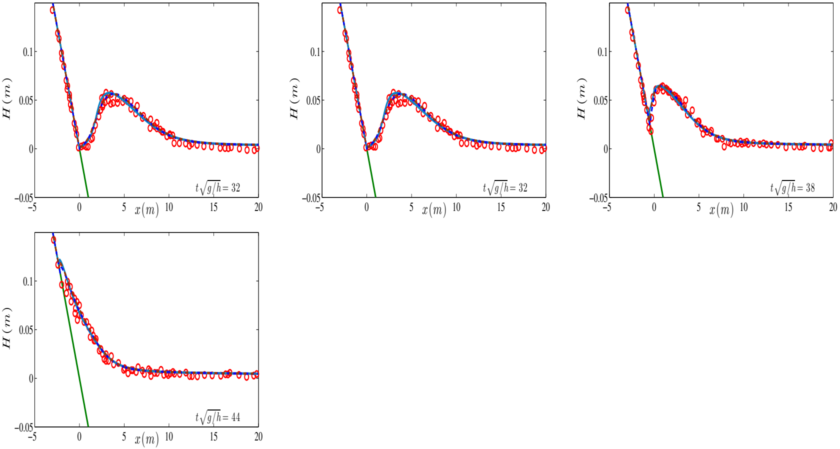

Solitary wave run-up on a plane beach

Area: $x \in [-20, 60m]$ $A/h = 0.04$, $Dx = 0.05$, $CFL = 0.4$, $n_m = 0.01$

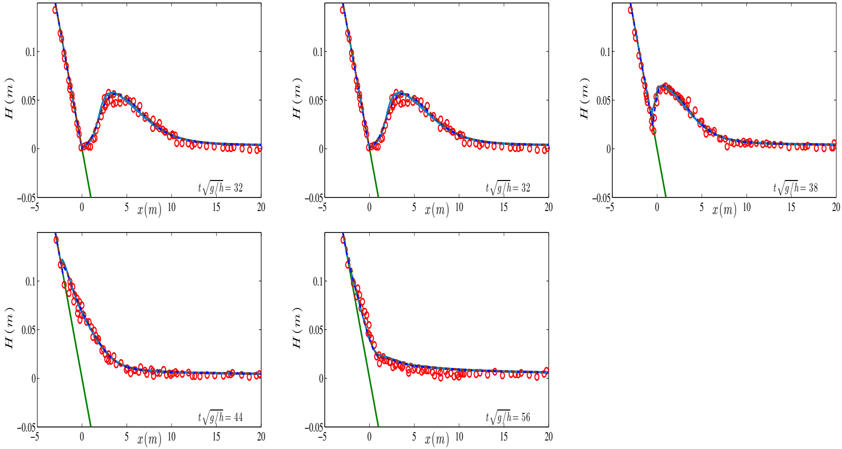

Solitary wave run-up on a plane beach

Area: $x \in [-20, 60m]$ $A/h = 0.04$, $Dx = 0.05$, $CFL = 0.4$, $n_m = 0.01$